12-2010

Mathematical Modeling, Simulation, and Time Series Analysis of Seasonal Epidemics.

Eric Shu Numfor
East Tennessee State University

Mathematical Modeling, Simulation, and Time Series Analysis of Seasonal Epidemics

---

A thesis

presented to

the faculty of the Department of Mathematics

East Tennessee State University

In partial fulfillment

of the requirements for the degree

Master of Science in Mathematical Sciences

---

by

Eric Numfor

December 2010

Ariel Cintrón-Arias, Ph.D., Chair

Jeff Knisley, Ph.D.

Robert Gardner, Ph.D.

Keywords: epidemics, basic reproduction number, seasonality, vaccination

ABSTRACT

Mathematical Modeling, Simulation, and Time Series Analysis of Seasonal Epidemics

by

Eric Numfor

Seasonal and non-seasonal Susceptible-Exposed-Infective-Recovered-Susceptible (SEIRS) models are formulated and analyzed. It is proved that the disease-free steady state of the non-seasonal model is locally asymptotically stable if $\mathcal{R}_v < 1$, and disease invades if $\mathcal{R}_v > 1$. For the seasonal SEIRS model, it is shown that the disease-free periodic solution is locally asymptotically stable when $\overline{\mathcal{R}}_v < 1$, and $I(t)$ is persistent with sustained oscillations when $\overline{\mathcal{R}}_v > 1$. Numerical simulations indicate that the orbit representing $I(t)$ decays when $\overline{\mathcal{R}}_v < 1 < \mathcal{R}_v$. The seasonal SEIRS model with routine and pulse vaccination is simulated, and results depict an unsustained decrease in the maximum of prevalence of infectives upon the introduction of routine vaccination and a sustained decrease as pulse vaccination is introduced in the population.

Mortality data of pneumonia and influenza is collected and analyzed. A decomposition of the data is analyzed, trend and seasonality effects ascertained, and a forecasting strategy proposed.

DEDICATION

This work is dedicated firstly to the Almighty God for His love, care, guidance and protection; secondly, to my wife, Agnes Shu, and kids, Ethel Shu and Klein Shu for their ever-ready support; and finally, to my mother, Mme Debora Lum for her encouragement.

ACKNOWLEDGMENTS

I would like to start off this page of acknowledgement by thanking the Almighty God who provided me the strength to pursue the difficult and turbulent route of academics.

Immense thanks are due to my advisor, Dr. Ariel Cintrón-Arias, firstly for providing me with the much-needed literature; secondly, for introducing me into this area of research and thirdly, for his patience, scientific counsel and enthusiasm. I am highly grateful to my professors, especially Drs. Robert Gardner, Debra Knisley, Jeff Knisley, Yared Nigussie, Anant Godbole and Teresa Haynes, who provided me the rudiments to pursue graduate studies at East Tennessee State University, and finally to the graduate coordinator and chair of the department for providing me with the much-needed financial assistantship.

Profound gratitude goes to Dr. Edith Seier, for introducing me into the area of Time Series Analysis and for her ever-ready support. I would say, I owe her a debt of gratitude.

May all the above mentioned people and others who remain anonymous here accept my heart-felt appreciation.

CONTENTS

LIST OF FIGURES

1 INTRODUCTION

Seasonal infections of humans range from childhood diseases, such as measles, chickenpox and diphtheria, acute diseases caused by the the bacteria *Carynebacterium diphtheriae*, to more faecal-oral infections such as cholera and rotaviruses, and vector-borne diseases including malaria [35]. Some of the causes of seasonality include [35]: the ability for the pathogen to survive outside the host, which depends on the temperature, humidity and exposure to sunlight; host immune function; the abundance of vectors and non-human hosts. The congregation of children during school terms has been demonstrated to influence annual variations in weekly incidence of a seasonal disease such as measles [32].

Although in 1760, Daniel Bernoulli formulated and solved a model for smallpox in order to evaluate the effectiveness of variolation of healthy people with the smallpox virus, deterministic epidemiological modeling seems to have started in the 20th century [37]. In 1906, Hamer [36] formulated and analyzed a discrete time model in an attempt to understand the recurrence of the outbreak of measles. Hamer's model may have been the first to assume the incidence (number of new cases per unit time) depends on the product of the densities of the susceptibles (individuals who can become infected) and infectives (infected individuals capable of transmitting the infection onto others). Ross [51] on the other hand, was interested in the incidence and control of malaria, so he developed differential equation models for malaria as a host-vector disease in 1911 [37]. Other deterministic epidemiological models were then developed in papers by Ross [51], Ross and Hudson [52], and Martini and Lotka [8, 19, 20]. In 1927, Kermack and McKendrick [40] published papers

on epidemic models and obtained the threshold result that the density of susceptibles must exceed a critical value in order for an epidemic outbreak to occur [8, 40]. Mathematical modeling seems to have grown in the middle of the 20th century with recent models involving aspects such as passive immunity, gradual loss of vaccine [3] and disease-acquired immunity, stages of infection, vertical transmission, disease vectors, vaccination, quarantine, social and sexual mixing groups and age structure [1, 2, 4, 11, 37].

The study of disease occurrence is called epidemiology, and an epidemic is an unusually large, but short-term outbreak of a disease [37]. A disease is called endemic if it persists in the population [37]. Emerging and reemerging diseases, such as influenza and pneumonia, have led to a revived interest in infectious diseases. The spread of infectious disease involves not only disease-related factors such as infectious agent, mode of transmission, latent period, infectious period, susceptibility and resistance, but also social, cultural, demographic, economic and geographic factors [37]. The model formulation process that we carry out in this thesis clarifies assumptions, variables and parameters, and the models provide conceptual results such as thresholds, basic reproduction number, transmissibility number and contact numbers [37]. Mathematical models and computer simulations are useful experimental tools for building and testing theories, assessing quantitative conjectures, answering specific questions and determining sensitivities to changes in parameter values. Mathematical modeling of seasonal epidemics can contribute to the design and analysis of epidemiological surveys, suggest crucial data to be collected, identify trends, make general forecasts and estimate uncertainty in forecasts [37].

In this thesis, we study seasonal epidemics, where we consider a general susceptible-exposed-infectious-recovered-susceptible (SEIRS) compartmental model. In this model, we assume forms for the transmission rate to have a non-seasonal SEIRS model, when the transmission rate is constant and a seasonal SEIRS model for a sinusoidal transmission rate. We assume that the transmission rate is

$$\beta(t) = \beta_0(1 + \beta_1 \cos(2\pi t)),$$

where β_0 is the baseline level of transmission, and β_1 is the strength of seasonality. When $\beta_1 \equiv 0$, the SEIRS model reduces to a non-seasonal model, while for $\beta_1 \in (0, 1)$, it reduces to a seasonal model. We incorporate pulse vaccination in these models and propose a strategy for disease control. In Chapter two, we derive and analyze seasonal and non-seasonal SEIRS models, and determine the basic reproduction number, steady states and stability analysis of the steady states. In Chapter three, we present numerical simulations and compare with the qualitative results from Chapter two. In Chapter four, we carry out a time series analysis of seasonal mortality data for influenza and pneumonia obtained from the Centers for Disease Control and Prevention (C.D.C.), by presenting some time series plots, periodogram, cumulative periodogram, decomposition plots, and carry out some forecasting strategy of time series data sets. In the last chapter, we make some concluding remarks.

2 MODEL AND ANALYSIS

The model we formulate here is an SEIRS model, where the population is divided into compartments containing susceptible, exposed, infectious and recovered individuals [7, 30, 37, 45, 47]. Compartments with labels S, E, I, R are used for epidemiological classes as shown in Figure 1. The class S is the class of susceptible individuals; that is, those who can become infected. When there is an adequate contact of a susceptible with an infective so that transmission occurs, the susceptible enters the exposed class E of those in the latent period, who are infected but not yet infectious. At the end of the latent period, the individual enters the class I of infectives, who are capable of transmitting the infection (that is, infectious). At the end of the infectious period, the individual enters the recovered class R. At time t, there are $S(t)$ susceptible, $E(t)$ exposed, $I(t)$ infectious and $R(t)$ recovered individuals in the population of constant size, N. The model assumes that all new-borns are susceptible (that is, no vertical transmission) to the infection and are recruited at rate μN. The susceptibles are exposed to the infection once in contact with an infectious individual. The exposed become infected at rate κE and the infectious individuals recover from the infection at rate γI. Recovered individuals who lose their immunity are recruited into the susceptible class at rate δR and the mortality rate for individuals in the different compartments is $\mu > 0$. This leads to Figure 1 that represents the transmission rate between classes of susceptible, exposed, infectious and recovered individuals in the population:

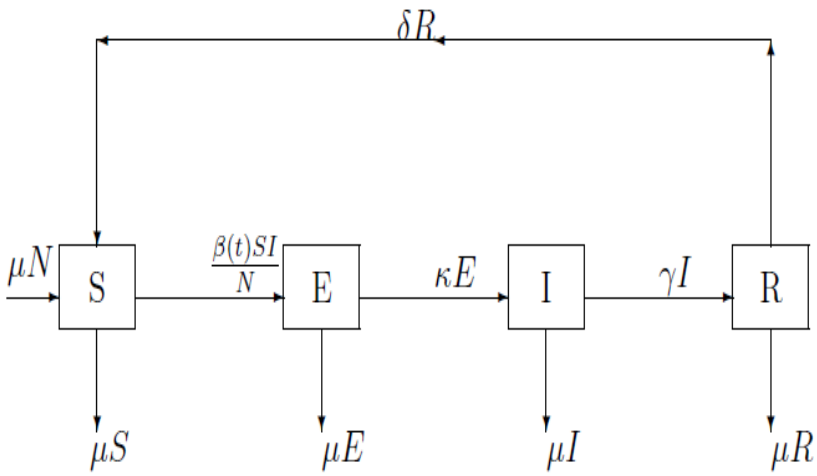

Figure 1: Schematic Diagram for SEIRS Model

From the compartmental diagram above, we have the following system of nonlinear ordinary differential equations that describe the spread of the infection in the population:

$$\begin{aligned}
\frac{dS}{dt} &= \mu N + \delta R(t) - \frac{\beta(t)S(t)I(t)}{N} - \mu S(t) \\
\frac{dE}{dt} &= \frac{\beta(t)S(t)I(t)}{N} - (\kappa + \mu)E(t) \\
\frac{dI}{dt} &= \kappa E(t) - (\gamma + \mu)I(t) \\
\frac{dR}{dt} &= \gamma I(t) - (\delta + \mu)R(t),
\end{aligned} \tag{1}$$

together with the following initial conditions:

$$S(t_0) = S_0, E(t_0) = E_0, I(t_0) = I_0, R(t_0) = N - S_0 - E_0 - I_0. \tag{2}$$

The parameters used in our model are defined as follows:

β denotes the transmission rate per of time,

γ denotes the per capita recovery rate per unit of time,

δ denotes the per capita rate of loss of immunity per unit of time,

κ denotes the per capita rate of active infection per unit of time,

μ denotes the per capita mortality rate per unit of time.

From the model, the rate of change of the total population with respect to time, $\frac{dN}{dt}$ is zero, thus the population at any time t is constant.

2.1 The Non-Seasonal SEIRS Model Without Vaccination

If the transmission rate $\beta(t) \equiv \beta_0$, where β_0 is constant, then the system of nonlinear ordinary differential equations (1) is autonomous [7], and is called the non-seasonal deterministic SEIRS model. Thus system (1) becomes:

$$\begin{aligned} \frac{dS}{dt} &= \mu N + \delta R(t) - \frac{\beta_0 S(t) I(t)}{N} - \mu S(t) \\ \frac{dE}{dt} &= \frac{\beta_0 S(t) I(t)}{N} - (\kappa + \mu) E(t) \\ \frac{dI}{dt} &= \kappa E(t) - (\gamma + \mu) I(t) \\ \frac{dR}{dt} &= \gamma I(t) - (\delta + \mu) R(t), \end{aligned} \tag{3}$$

together with initial conditions defined in equation (2).

2.1.1 The Basic Reproduction Number $\mathcal{R}_0$

The basic reproduction number, $\mathcal{R}_0$, is a key concept in epidemiology, and one of the foremost and most valuable ideas that mathematical thinking brought to epidemic

theory [25, 26]. The basic reproduction number was originally developed for the study of demographics (Sharp and Lotka 1911 [55], Dublin and Lotka 1925 [24]) but was independently studied for vector-borne diseases such as malaria (Ross 1911 [51], MacDonald 1952 [46]) and directly transmitted human infections (Kermack and McKendrick 1927 [40]). It is now widely used for the study of infectious diseases.

The basic reproduction number, $\mathcal{R}_0$, for a non-seasonal infection is defined as the number of secondary infections that result from the introduction of a single infectious individual into a completely susceptible population during its entire period of infectiousness [11, 15, 14, 23, 26, 27, 30, 45]. The basic reproduction number provides an invasion criterion for the initial spread of the infection in a susceptible population. Also, it measures the transmissibility of a pathogen and determines the magnitude of public health intervention necessary to control epidemics [14]. If $\mathcal{R}_0 < 1$, then on the average, an infected individual produces less than one new infected individual over the course of its infectious period, and the infection cannot spread [23]. On the other hand, if $\mathcal{R}_0 > 1$, then each infected individual produces, on the average, more than one new infection, and the disease can invade the population. When $\mathcal{R}_0 = 1$, a transcritical bifurcation occurs [11]; that is, asymptotic local stability is transferred from the infectious-free state to the new (emerging) endemic state.

One way of calculating the basic reproduction number, $\mathcal{R}_0$, is by the *next generation operator approach* [11, 23, 26, 27]. A rich history in the literature addresses the derivation of $\mathcal{R}_0$, or equivalent threshold parameter when more than one class of infectives is involved. The next generation method, introduced by Diekmann *et al.* [18], is a generation method of deriving $\mathcal{R}_0$ in such cases, encompassing any situation

in which the population is divided into discrete, disjoint classes of the form [11]:

$$\begin{aligned} \frac{dX}{dt} &= f(X,Y,Z) \\ \frac{dY}{dt} &= g(X,Y,Z) \\ \frac{dZ}{dt} &= h(X,Y,Z), \end{aligned}$$

where $X \in \Re^u$, $Y \in \Re^v$, $Z \in \Re^w$ and $h(X,0,0) = 0$. Here, the components of X denote the number of susceptibles, recovered, and other classes of non-infected individuals. The components of Y denote the number of infected individuals who do not transmit the disease (such as the latent and non-infectious stages), and the components of Z represent the number of infected individuals capable of transmitting the disease (such as the infectious and non-quarantined individuals) [43]. We let $(X^*,0,0) \in \Re^{u+v+w}$ denotes the disease-free equilibrium. That is,

$$f(X^*,0,0) = g(X^*,0,0) = h(X^*,0,0) = 0,$$

and assume that the equation $g(X^*,Y,Z) = 0$ implicity defines the function $Y = \tilde{g}(X^*,Y)$, and

$$A = D_Z h(X^*, \tilde{g}(X^*,0),0).$$

Further, we assume that A can be written in the form $A = M - D$, where the matrix $M = (m_{ij}) \geq 0$ and D is a diagonal matrix. Thus, the basic reproduction number is defined as the spectral radius (dominant eigenvalue) of the matrix MD^{-1}; that is,

$$\mathcal{R}_0 = \rho(MD^{-1}),$$

where the resolvent of any matrix A is $\rho(A) = max\{|\lambda|, \lambda \in sp(A)\}$, the spectrum of A is $sp(A) = \{\lambda_i, i = 1,2,...n\}$ and λ_i is an eigenvalue of A [17]. By the next

generation approach, we have the following basic reproduction number for system (3):

$$\mathcal{R}_0 = \beta_0 \frac{\kappa}{\mu+\kappa} \frac{1}{\mu+\gamma}. \tag{4}$$

The basic reproduction number (4) is the product of the constant transmission rate, β_0, per unit time t, the average infectious period adjusted for population growth, $\frac{1}{(\mu+\gamma)}$, and the fraction $\frac{\kappa}{(\mu+\kappa)}$ of the exposed individuals surviving the exposed class, E [10, 37]. Thus, $\mathcal{R}_0$ is suitably expressed as the average of the number of secondary infections that result from the introduction of an infectious individual in a susceptible population during its entire period of infectiousness.

2.1.2 Existence of Steady States

We eliminate one of the state variables by setting $R(t) = N - S(t) - E(t) - I(t)$, to have the following 3-dimensional system:

$$\begin{aligned}
\frac{dS}{dt} &= (\mu+\delta)N - \frac{\beta_0 S(t) I(t)}{N} - (\mu+\delta)S(t) - \delta E(t) - \delta I(t) \\
\frac{dE}{dt} &= \frac{\beta_0 S(t) I(t)}{N} - (\kappa+\mu)E(t) \\
\frac{dI}{dt} &= \kappa E(t) - (\gamma+\mu)I(t)
\end{aligned} \tag{5}$$

The steady states of system (5) are obtained by setting $\frac{dS}{dt} = \frac{dE}{dt} = \frac{dI}{dt} = 0$. This yields the disease-free equilibrium $(S^0, E^0, I^0) = (N, 0, 0)$ and the endemic equilibrium $(\overline{S}, \overline{E}, \overline{I})$, where

$$
\begin{aligned}
\overline{S} &= \frac{N}{\mathcal{R}_0}, \\
\overline{E} &= \frac{N(\mu+\gamma)(\mu+\delta)}{\mathcal{R}_0(\kappa+\delta(\mu+\gamma)+\delta\kappa)}\left(\mathcal{R}_0-1\right), \\
\overline{I}_0 &= \frac{N\kappa(\mu+\delta)}{\mathcal{R}_0(\kappa+\delta(\mu+\gamma)+\delta\kappa)}\left(\mathcal{R}_0-1\right).
\end{aligned} \tag{6}
$$

The endemic equilibrium point exists when $\mathcal{R}_0 > 1$ and is unrealistic when $\mathcal{R}_0 < 1$, because $\overline{E} < 0$ and $\overline{I} < 0$. When $\mathcal{R}_0 = 1$, the endemic equilibrium reduces to the disease-free equilibrium.

2.1.3 Linear Stability Analysis

The stability analysis of the disease-free and endemic equilibria are governed by the eigenvalues of the Jacobian matrix of system (5), evaluated at these points. For stability, we require that $Re(\lambda) < 0$, where λ is an eigenvalue of the linearized system evaluated at the respective steady states [47].

Theorem 2.1 *The disease-free equilibrium (S^0, E^0, I^0), is locally asymptotically stable when $\mathcal{R}_0 < 1$. Moreover, the endemic equilibrium $(\overline{S}, \overline{E}, \overline{I})$, is locally asymptotically stable when $\mathcal{R}_0 > 1$.*

Proof: The stability of the disease-free and endemic equilibria are determined by the following Jacobian matrix of system (5):

$$A = \begin{pmatrix} \frac{\beta_0 I}{N} - (\mu+\delta) & -\delta & \frac{\beta_0 S}{N} - \delta \\ \frac{\beta_0 I}{N} & -(\mu+\kappa) & \frac{\beta_0 S}{N} \\ 0 & \kappa & -(\mu+\gamma) \end{pmatrix}. \tag{7}$$

At the disease-free equilibrium $(N, 0, 0)$, the equation $|A - \lambda I| = 0$ yields a third degree polynommial in λ of the form:

$$P(\lambda) = \lambda^3 + a_1\lambda^2 + a_2\lambda + a_3, \tag{8}$$

where $a_i = a_i(\mathcal{R}_0)$ is given by

$$\begin{aligned} a_1(\mathcal{R}_0) &= 3\mu + \kappa + \gamma + \delta, \\ a_2(\mathcal{R}_0) &= (\mu+\delta)(2\mu+\kappa+\delta) + (\mu+\kappa)(\mu+\gamma)(1-\mathcal{R}_0), \\ a_3(\mathcal{R}_0) &= (\mu+\kappa)(\mu+\gamma)(\mu+\delta)(1-\mathcal{R}_0). \end{aligned}$$

By the Routh-Hurwitz condition [47], we require that $a_3 > 0$, $D_1 = a_1 > 0$ and $D_2 = a_1a_2 - a_3 > 0$, for the eigenvalues (that is, roots of (8)) to have negative real parts. Thus,

$$\begin{aligned} a_3 &= (\mu+\kappa)(\mu+\gamma)(\mu+\delta)(1-\mathcal{R}_0), \\ D_1 &= 3\mu + \kappa + \gamma + \delta, \\ D_2 &= (2\mu+\kappa+\gamma)(\mu+\kappa)(\mu+\gamma)(1-\mathcal{R}_0) \\ &\quad +(3\mu+\kappa+\gamma+\delta)(2\mu+\kappa+\delta)(\mu+\delta). \end{aligned}$$

The parameter $D_1 > 0$, while a_3 and D_2 are positive if $\mathcal{R}_0 < 1$. Thus, when $\mathcal{R}_0 < 1$, the Routh-Hurwitz conditions are satisfied and the eigenvalues have negative real

parts, and the disease-free equilibrium is locally asymptotically stable. Hence, the disease gradually disappears from the population. When $\mathcal{R}_0 > 1$, the disease persist in the population (there exists a non-zero endemic equilibrium). At the endemic equilibrium point, the equation $|A - \lambda I| = 0$ yields the cubic polynomial

$$Q(\lambda) = \lambda^3 + b_1\lambda^2 + b_2\lambda + b_3, \tag{9}$$

where $b_i = b_i(\mathcal{R}_0)$ is given by:

$$\begin{aligned}
b_1(\mathcal{R}_0) &= 2\mu + \kappa + \gamma + \left(\frac{(\mu+\kappa)(\mu+\gamma)(\mu+\delta)}{\kappa + \delta(\mu+\gamma) + \delta\kappa}\right)(\mathcal{R}_0 - 1), \\
b_2(\mathcal{R}_0) &= (\mu+\delta)(2\mu+\kappa+\gamma+\delta)(\mu+\kappa)\left(\frac{(\mu+\kappa)(\mu+\gamma)(\mu+\delta)}{\kappa + \delta(\mu+\gamma) + \delta\kappa}\right)(\mathcal{R}_0 - 1), \qquad (10) \\
b_3(\mathcal{R}_0) &= (\delta(\mu+\gamma) + (\mu+\kappa)(\mu+\gamma)(\mu+\delta) + \delta\kappa)\left(\frac{(\mu+\kappa)(\mu+\gamma)(\mu+\delta)}{\kappa + \delta(\mu+\gamma) + \delta\kappa}\right)(\mathcal{R}_0 - 1).
\end{aligned}$$

As above, we determine expressions for D_1 and $D_2 = b_1b_2 - b_3$. Notice that $D_1 = b_1$ given in (10) above. So, we only determine an expression for D_2. Now,

$$\begin{aligned}
D_2 &= ((\mu+\kappa)(2\mu+\kappa+\gamma) + (\mu+\gamma)^2 + \delta\mu)\left(\frac{(\mu+\kappa)(\mu+\gamma)(\mu+\delta)(\mathcal{R}_0-1)}{\kappa + \delta(\mu+\gamma) + \delta\kappa}\right) \\
&\quad + (2\mu+\kappa+\gamma+\delta)\left(\frac{(\mu+\kappa)(\mu+\gamma)(\mu+\delta)(\mathcal{R}_0-1)}{\kappa + \delta(\mu+\gamma) + \delta\kappa}\right)^2. \qquad (11)
\end{aligned}$$

If $\mathcal{R}_0 > 1$, the parameter b_3 given in equation (10) is positive, and D_1 and D_2 are also positive. Thus, when $\mathcal{R}_0 > 1$, the Routh-Hurwitz conditions are again satisfied. Thus all eigenvalues obtained from equation (9) have negative real parts. Hence, the endemic equilibrium is locally asymptotically stable when $\mathcal{R}_0 > 1$. □

2.2 SEIRS Non-Seasonal Model With Vaccination

The study of vaccination in the transmission of infectious diseases has been of intense theoretical analysis [38, 49, 53]. Routine vaccination of a fraction of the pop-

ulation at or soon after birth increases the mean age at infection in a homogeneous population, and thus increases the natural period of the non-seasonal endemic dynamics [35]. Pulse vaccination, on the other hand, is an articulate strategy for the elimination of infectious diseases, such as measles and polio [35]. It consists of periodical repetitions of impulsive vaccinations in the population, on all the age groups. This kind of vaccination is called pulse since all the vaccine doses are applied in a very short time with respect to the dynamics of the target disease [22]. Here, we model pulse vaccination as a transfer of vaccinated individuals from the susceptible class directly to the recovered class, at rate ξS. In the recovered class, individuals either die at rate μR or become susceptible to the infection at rate δR. This leads to Figure 2 that represents the transmission rate between classes of susceptible, exposed, infectious and recovered individuals in the population:

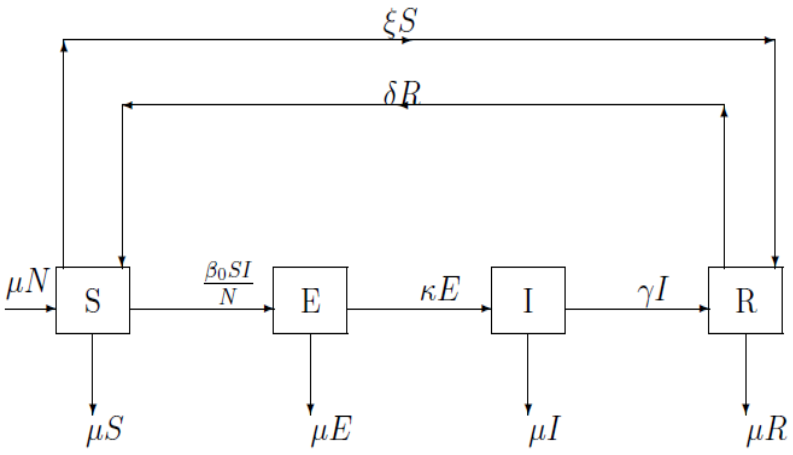

Figure 2: Schematic Diagram for SEIRS Model with Pulse Vaccination

As in Figure 1, we obtain the following system of ordinary differential equations from

Figure 2.

$$\begin{aligned}
\frac{dS}{dt} &= \mu N + \delta R(t) - \frac{\beta_0 S(t) I(t)}{N} - (\mu + \xi) S(t) \\
\frac{dE}{dt} &= \frac{\beta_0 S(t) I(t)}{N} - (\kappa + \mu) E(t) \\
\frac{dI}{dt} &= \kappa E(t) - (\gamma + \mu) I(t) \\
\frac{dR}{dt} &= \gamma I(t) + \xi S(t) - (\delta + \mu) R(t),
\end{aligned} \tag{12}$$

with initial conditions defined in equation (2). Assuming $\xi(t) \equiv \xi_0$ constant and applying the next generation operator approach, we have the vaccination basic reproduction number $\mathcal{R}_v$, as follows:

$$\mathcal{R}_v = \frac{\beta_0 \kappa (\mu + \delta)}{(\mu + \kappa)(\mu + \gamma)(\mu + \delta + \xi_0)}. \tag{13}$$

The basic reproduction number $\mathcal{R}_v$, reduces to the basic reproduction number $\mathcal{R}_v$, given in equation (4) if $\xi_0 = 0$. Now, we eliminate one of the state variables in equation (12) by setting $R(t) = N - S(t) - E(t) - I(t)$. This leads to the following system of nonlinear ordinary differential equations describing the spread of an epidemic in a population with routine vaccination:

$$\begin{aligned}
\frac{dS}{dt} &= (\mu + \delta) N - \frac{\beta_0 S(t) I(t)}{N} - (\mu + \delta + \xi) S(t) - \delta E(t) - \delta I(t) \\
\frac{dE}{dt} &= \frac{\beta_0 S(t) I(t)}{N} - (\kappa + \mu) E(t) \\
\frac{dI}{dt} &= \kappa E(t) - (\gamma + \mu) I(t)
\end{aligned} \tag{14}$$

Deriving analogous results to those obtained in Section 2.1.2, we have the disease-free

equilibrium

$$(S^0, E^0, I^0) = \left(\frac{N(\mu+\delta)}{\mu+\delta+\xi}, 0, 0 \right), \tag{15}$$

and the endemic equilibrium $(\overline{S}, \overline{E}, \overline{I})$, where

$$\begin{aligned}
\overline{S} &= \frac{N(\mu+\delta)}{(\mu+\delta+\xi)\mathcal{R}_v}, & (16)\\
\overline{E} &= \left(\frac{N(\mu+\kappa)(\mu+\gamma)^2(\mu+\delta+\xi)}{\kappa(\kappa(\mu+\kappa)(\mu+\gamma)+\delta(\mu+\gamma)+\delta\kappa)} \right)(\mathcal{R}_v - 1), & (17)\\
\overline{I} &= \left(\frac{N(\mu+\kappa)(\mu+\gamma)(\mu+\delta+\xi)}{\kappa(\mu+\kappa)(\mu+\gamma)+\delta(\mu+\gamma)+\delta\kappa} \right)(\mathcal{R}_v - 1). & (18)
\end{aligned}$$

Theorem 2.2 *The disease-free equilibrium (S^0, E^0, I^0), is locally asymptotically stable when $\mathcal{R}_v < 1$. Moreover, the endemic equilibrium $(\overline{S}, \overline{E}, \overline{I})$, is locally asymptotically stable when $\mathcal{R}_v > 1$.*

Proof: The stability of equilibria is determined by the Jacobian matrix

$$B = \begin{pmatrix} \frac{\beta_0 I}{N} - (\mu+\delta+\xi) & -\delta & \frac{\beta_0 S}{N} - \delta \\ \frac{\beta_0 I}{N} & -(\mu+\kappa) & \frac{\beta_0 S}{N} \\ 0 & \kappa & -(\mu+\gamma) \end{pmatrix}. \tag{19}$$

At the disease-free steady state (15), $|B - \lambda I| = 0$ yields the following third degree polynomial in λ:

$$F(\lambda) = \lambda^3 + c_1\lambda^2 + c_2\lambda + c_3, \tag{20}$$

where $c_i = c_i(\mathcal{R}_v)$ is given by

$$\begin{aligned}
c_1(\mathcal{R}_v) &= 3\mu + \kappa + \gamma + \delta + \xi,\\
c_2(\mathcal{R}_v) &= (\mu+\delta+\xi)(2\mu+\kappa+\delta) + (\mu+\kappa)(\mu+\gamma)(1-\mathcal{R}_v),\\
c_3(\mathcal{R}_v) &= (\mu+\kappa)(\mu+\gamma)(\mu+\delta+\xi)(1-\mathcal{R}_v).
\end{aligned}$$

Now, the coefficient $c_3 > 0$ if $\mathcal{R}_v < 1$ and $D_1 = c_1 > 0$, with

$$\begin{aligned} D_2 &= c_1c_2 - c_3 \\ &= (3\mu+\kappa+\gamma+\delta+\xi)(\mu+\delta+\xi)(2\mu+\kappa+\gamma) + (\mu+\kappa)(\mu+\gamma)(1-\mathcal{R}_v) \\ &\quad -(\mu+\kappa)(\mu+\gamma)(\mu+\delta+\xi)(1-\mathcal{R}_v) \\ &= (\mu+\delta+\xi)((\mu+\kappa)(\mu+\gamma) + (2\mu+\kappa+\gamma)(2\mu+\kappa+\delta+\xi) + (\mu+\gamma)^2) \\ &\quad +(\mu+\kappa)(\mu+\gamma)(2\mu+\kappa+\gamma)(1-\mathcal{R}_v). \end{aligned}$$

The parameter $D_2 > 0$ if $\mathcal{R}_v < 1$. Thus, the Routh Hurwitz conditions are satisfied and hence the disease-free equilibrium is locally asymptotically stable when $\mathcal{R}_v < 1$. At the endemic equilibrium, $|B - \lambda I| = 0$ leads to the polynomial

$$G(\lambda) = \lambda^3 + d_1\lambda^2 + d_2\lambda + d_3, \tag{21}$$

where $d_i = d_i(\mathcal{R}_v)$ is given by

$$\begin{aligned} d_1(\mathcal{R}_v) &= 3\mu+\kappa+\gamma+\delta+\xi + \frac{\beta_0(\mu+\kappa)(\mu+\gamma)(\mu+\delta+\xi)(\mathcal{R}_v-1)}{\kappa(\mu+\kappa)(\mu+\gamma)+\delta(\mu+\gamma)+\delta\kappa}, \\ d_2(\mathcal{R}_v) &= (\mu+\delta+\xi)(2\mu+\kappa+\gamma) \\ &\quad + \frac{\beta_0(2\mu+\kappa+\gamma+1)(\mu+\kappa)(\mu+\gamma)(\mu+\delta+\xi)(\mathcal{R}_v-1)}{\kappa(\mu+\kappa)(\mu+\gamma)+\delta(\mu+\gamma)+\delta\kappa}, \\ d_3(\mathcal{R}_v) &= \beta_0(\delta(\mu+\gamma)+(\mu+\kappa)(\mu+\gamma)+\delta\gamma)\left(\frac{(\mu+\kappa)(\mu+\gamma)(\mu+\delta+\xi)(\mathcal{R}_v-1)}{\kappa(\mu+\kappa)(\mu+\gamma)+\delta(\mu+\gamma)+\delta\kappa}\right). \end{aligned}$$

The coefficients of the characteristic polynomial (21) are positive if $\mathcal{R}_v > 1$. Thus,

when $\mathcal{R}_v > 1$, $d_3 > 0$, $D_1 = d_1 > 0$ and

$$\begin{aligned} D_2 &= d_1 d_2 - d_3 \\ &= s + (2\mu + \kappa + \gamma + 1)\left(\frac{\beta_0(\mu+\kappa)(\mu+\gamma)^2(\mu+\delta+\xi)}{\kappa(\mu+\kappa)(\mu+\gamma)+\delta(\mu+\gamma)+\delta\kappa}(\mathcal{R}_v - 1)\right)^2 \\ &\quad +(u+v+w)\left(\frac{\beta_0(\mu+\kappa)(\mu+\gamma)^2(\mu+\delta+\xi)}{\kappa(\mu+\kappa)(\mu+\gamma)+\delta(\mu+\gamma)+\delta\kappa}\right)(\mathcal{R}_v - 1) > 0, \end{aligned}$$

where

$$\begin{aligned} s &= (3\mu + \kappa + \delta + \gamma + \xi)(\mu + \delta + \xi)(2\mu + \kappa + \gamma) > 0, \\ u &= 2\mu + \delta + \gamma + \xi > 0, \\ v &= (2\mu + \kappa + \gamma)(3\mu + \delta + \gamma + 2\xi) > 0, \\ w &= (\mu + \kappa)(\mu + \gamma + 1) + \delta\kappa > 0. \end{aligned}$$

Thus, the endemic equilibrium is locally asymptotically stable when $\mathcal{R}_v > 1$. □

2.3 The Seasonal SEIRS Model Without Vaccination

For mathematical convenience, seasonal transmissions are often assumed to be sinusoidal [35], such that the transmission parameter is a time dependent function defined by

$$\beta(t) = \beta_0(1 + \beta_1 \cos(2\pi t)), \tag{22}$$

where β_0 is the baseline level of transmission and β_1 is the amplitude of seasonal variation or the strength of seasonality (seasonal forcing) [35]. In Figure 3, the baseline transmission is $\beta_0 = 4$ and amplitude of seasonality is $\beta_1 = 0.0283$. The graph of $\beta(t)$ depicts a periodic curve with period 1 and amplitude $\beta_0\beta_1$.

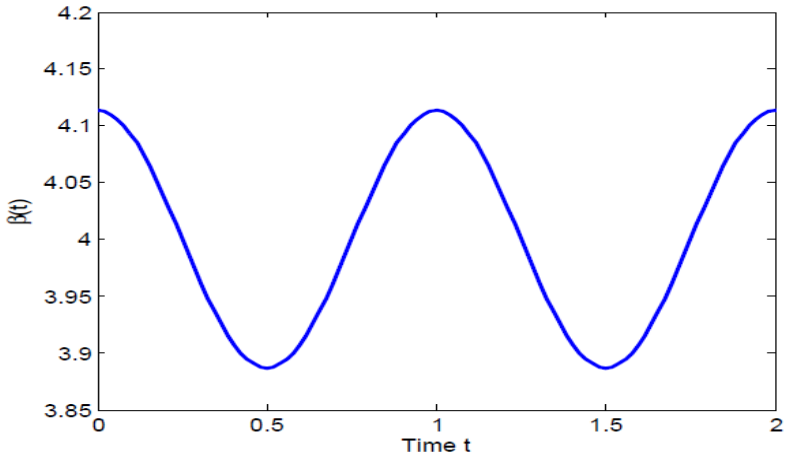

Figure 3: Sinusoidal Transmission Rate Against Time t

Thus, the seasonal SEIRS model corresponding to the non-seasonal model (3) is:

$$\begin{aligned}
\frac{dS}{dt} &= \mu N + \delta R(t) - \frac{\beta(t)S(t)I(t)}{N} - \mu S(t) \\
\frac{dE}{dt} &= \frac{\beta(t)S(t)I(t)}{N} - (\kappa + \mu)E(t) \\
\frac{dI}{dt} &= \kappa E(t) - (\gamma + \mu)I(t) \\
\frac{dR}{dt} &= \gamma I(t) - (\delta + \mu)R(t),
\end{aligned} \tag{23}$$

where $\beta(t) = \beta_0(1+\beta_1\cos(2\pi t))$, $0 < \beta_1 < 1$, with initial conditions given in equation (2).

2.3.1 The Transmissibility Number $\overline{\mathcal{R}}_0$

The transmissibility number for seasonal epidemics is interpreted differently from the basic reproduction number for a non-seasonal epidemics. The basic reproduction

number for a non-seasonal epidemic represents the number of secondary infections that result from the introduction of a single infectious individual in an entirely susceptible population. This interpretation is not possible for a seasonal epidemics, since the number of secondary infections will depend on the time of the year that the infectious individual is introduced into the population. Thus, the transmissibility number, $\overline{\mathcal{R}}_0$, for a seasonal epidemic is defined as the *average* number of secondary cases arising from the introduction of a single infectious person into a completely susceptible population at a *random* time of the year [35]. Thus, deriving an expression for $\overline{\mathcal{R}}_0$ that has a similar interpretation to $\mathcal{R}_0$ requires averaging over all possible times of the year that an infection may be introduced [35]. As in equation (5), we eliminate one of the state variables in equation (23) to have the following system of ordinary differential equations:

$$\begin{aligned}
\frac{dS}{dt} &= (\mu+\delta)N - \frac{\beta(t)S(t)I(t)}{N} - (\mu+\delta)S(t) - \delta E(t) - \delta I(t) \\
\frac{dE}{dt} &= \frac{\beta(t)S(t)I(t)}{N} - (\kappa+\mu)E(t) \\
\frac{dI}{dt} &= \kappa E(t) - (\gamma+\mu)I(t),
\end{aligned} \tag{24}$$

where $\beta(t) = \beta_0(1+\beta_1\cos(2\pi t))$, $0 < \beta_1 < 1$. By linearizing system (24) near the disease-free steady state $(N, 0, 0)$, we have:

$$\begin{aligned}
\frac{dE}{dt} &= \beta(t)I - (\mu+\kappa)E \\
\frac{dI}{dt} &= \kappa E - (\mu+\gamma)I
\end{aligned} \tag{25}$$

The transmissibility number $\overline{\mathcal{R}}_0$ is defined through the spectral radius of a linear integral operator on a space of periodic functions as proposed by Bacaer [5]. In this

case, we let $t \in \Re$ and $x \geq 0$, so that the operator $K(t,x) = K_{ij}(t,x)$ is an epidemic model with two infected classes, $(I_1, I_2) = (E, I)$. Here, the coefficient $K_{ij}(t,x)$ in row i, column j represents the expected number of individuals in compartment I_i that one individual in compartment I_j generates at the beginning of an epidemic per unit time at time t if it has been in compartment I_j for x units of time. This yields

$$\begin{aligned} K(t,x) &= \begin{pmatrix} k_{11} & k_{12} \\ k_{21} & k_{22} \end{pmatrix} \\ &= \begin{pmatrix} 0 & \beta(t)e^{-(\mu+\gamma)x} \\ \kappa e^{-(\mu+\kappa)x} & 0 \end{pmatrix} \end{aligned}$$

Thus, the integral operator G_j is defined by

$$G_j = \left(\int_0^\infty g_1 e^{-2\pi jix} dx \right) ... \left(\int_0^\infty g_n e^{-2\pi jix} dx \right),$$

where g_j is defined by $g_j = a_j e^{-b_j x}$ for $1 \leq j \leq n$. This yields

$$\begin{aligned} G_j &= \left(\int_0^\infty \beta_0 e^{-(\mu+\gamma)x} e^{-2\pi jix} dx \right) \left(\int_0^\infty \kappa e^{-(\mu+\kappa)x} e^{-2\pi jix} dx \right) \\ &= \frac{\beta_0 \kappa}{(\mu + \kappa + 2\pi ij)(\mu + \gamma + 2\pi ij)}, \end{aligned}$$

so that

$$\begin{aligned} G_0 &= \frac{\beta_0 \kappa}{(\mu + \kappa)(\mu + \gamma)}, \\ G_1 &= \frac{\beta_0 \kappa}{(\mu + \kappa + 2\pi i)(\mu + \gamma + 2\pi i)}. \end{aligned}$$

Thus, as proposed by Bacaer (2007), the transmissibility number $\overline{\mathcal{R}}_0$ is determined from [5, 6] as:

$$\overline{\mathcal{R}}_0 = G_0 + \frac{\beta_1^2}{2} Re \left(\frac{G_0 G_1}{G_0 - G_1} \right),$$

where $Re(.)$ is the real part of $(.)$. We thus obtain

$$\overline{\mathcal{R}}_0 = \frac{\beta_0\kappa}{(\mu+\kappa)(\mu+\gamma)} + \frac{\beta_1^2}{2} Re\left[\frac{\left(\frac{\beta_0\kappa}{(\mu+\kappa)(\mu+\gamma)}\right)\left(\frac{1}{(\mu+\kappa+2\pi i)(\mu+\gamma+2\pi i)}\right)}{\left(\frac{1}{(\mu+\kappa)(\mu+\gamma)}\right) - \left(\frac{1}{(\mu+\kappa+2\pi i)(\mu+\gamma+2\pi i)}\right)}\right],$$

which yields the transmissibility number for the seasonal model as [5, 61]

$$\overline{\mathcal{R}}_0 = \frac{\beta_0\kappa}{(\mu+\kappa)(\mu+\gamma)}\left[1 - \frac{(\mu+\kappa)(\mu+\gamma)}{4\pi^2 + (2\mu+\kappa+\gamma)^2}\frac{\beta_1^2}{2}\right]. \tag{26}$$

The first term in (26) is the basic reproduction number for the non-seasonal model (3), obtained when $\beta_1 = 0$. From (26), we notice that

$4\pi^2 + (2\mu+\kappa+\gamma)^2 = 4\pi^2 + ((\mu+\kappa)+(\mu+\gamma))^2 > (\mu+\kappa)(\mu+\gamma)$, so that

$$\frac{(\mu+\kappa)(\mu+\gamma)}{4\pi^2 + (2\mu+\kappa+\gamma)^2}\frac{\beta_1^2}{2} < \frac{\beta_1^2}{2} < 1.$$

Thus, the size of $\overline{\mathcal{R}}_0$ is reduced compared to $\mathcal{R}_0$ when the transmission rate is constant, and this makes it slightly difficult for the parasite to invade the population with such fluctuations in $\beta(t)$ [5]. Unlike in a non-seasonal epidemic where the condition $\mathcal{R}_0 < 1$ indicates that the infection dies out of the population, in a seasonal epidemic, the condition $\overline{\mathcal{R}}_0 < 1$ is not sufficient to prevent an outbreak, since chains of transmission can be established during high seasons, but it is necessary and sufficient for long-term disease eradication [35].

2.4 SEIRS Seasonal Model With Vaccination

Customary to the non-seasonal SEIRS model with routine vaccination, we notice that the system of equations for the non-seasonal model for which the transmission rate is a time dependent function defined by $\beta(t) = \beta_0(1 + \beta_1\cos(2\pi t))$, $\beta_1 \in (0, 1)$ is called the seasonal SEIRS model with pulse vaccinations. In the derivation of the

seasonal model with pulse vaccination, we partition the susceptible class into the vaccinated and unvaccinated individuals, denoted $\tilde{S}_v$ and $\tilde{S}$ respectively. In this case, the total population is given by $N = \tilde{S}_v(t) + \tilde{S}(t) + E(t) + I(t) + R(t)$, with the susceptibles given by $S(t) = \tilde{S}_v(t) + \tilde{S}(t)$. This leads to the following model that describes the spread of a seasonal infection with pulse vaccination.

$$\begin{aligned}
\frac{dS}{dt} &= \mu N + \delta R(t) - \frac{\beta(t)S(t)I(t)}{N} - (\mu + \xi_0)S(t) \\
\frac{dE}{dt} &= \frac{\beta(t)S(t)I(t)}{N} - (\kappa + \mu)E(t) \\
\frac{dI}{dt} &= \kappa E(t) - (\gamma + \mu)I(t) \\
\frac{dR}{dt} &= \gamma I(t) + \xi_0 S(t) - (\delta + \mu)R(t),
\end{aligned} \tag{27}$$

where $\beta(t) = \beta_0(1 + \beta_1 cos(2\pi t))$, with $\beta_1 \in (0, 1)$. Since the total population is $N = \tilde{S}_v(t) + \tilde{S}(t) + E(t) + I(t) + R(t)$, we have $\frac{\tilde{S}}{N} = 1 - \left(\frac{\tilde{S}_v(t)}{N} + \frac{E(t)}{N} + \frac{I(t)}{N} + \frac{R(t)}{N}\right)$, so that the fraction, $Q(\tau)$, of the population that remains unvaccinated at time τ is

$$Q(\tau) = 1 - \left(\frac{\tilde{S}_v(\tau) + E(\tau) + I(\tau) + R(\tau)}{N}\right). \tag{28}$$

Since the transmissibility number, $\overline{R}_v$, of a seasonal model is interpreted as the *average* number of secondary cases arising from the introduction of a single infected person into a completely susceptible population at a *random time* of the year, we define $\overline{\mathcal{R}}_v$ for system (27) as:

$$\overline{\mathcal{R}}_v(t) = \frac{\kappa(\mu + \delta)}{(\mu + \kappa)(\mu + \gamma)(\mu + \delta + \xi_0)} \int_{t_0}^{t} \beta(\tau)Q(\tau)d\tau, \tag{29}$$

where $\beta(\tau)$ and $Q(\tau)$ are defined in equations (24) and (28), respectively. Since the fraction of the unvaccinated individuals, $Q(\tau)$ depends on the solutions, S, E, I and R, obtained from system (27) numerically, we determine $\overline{\mathcal{R}}_v(t)$ numerically. Using a MATLAB built-in function *trapz*, that implements quadrature rule [29] and representing a plot of the solution, we obtain Figure 5 below, which depicts a sinusoidal transmissibility number for any given time t. The transmissibility number, $\overline{\mathcal{R}}_v(t)$ at time t years, is thus obtained as the average of the transmissibility numbers from t_0 to t during which the infection may have been introduced.

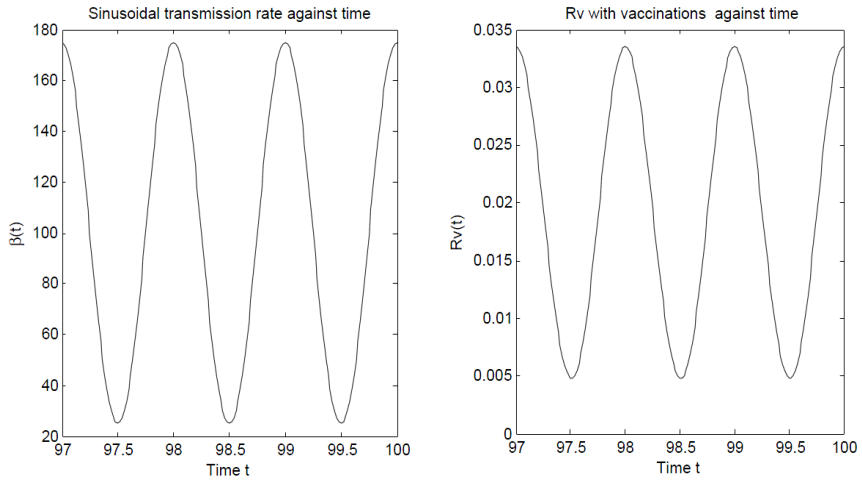

Figure 4: Relationship Between the Transmission Rate and the Transmissibility Number, $\mathcal{R}_v$

In Figure 4, a decrease in the transmission rate results in a decrease in the transmissibility number and an increase in the transmission rate results in an increase in the transmissibility number. Thus, the sum of the transmissibility numbers from time t_0 years to any given time of the year gives the number of secondary cases that result

from the introduction of a single infectious individual into a completely susceptible population at that given time of the year. The sum of the transmissibility number is below unity at all times. This suggests that the form of the transmissibility number (26) proposed by Grassly and Fraser [35] is not a good representation of the transmissibility number for our model. Thus, we assume that $\xi(t) = \xi_0$ and linearize system (27) about the disease-free steady state $\left(\frac{N(\mu+\delta)}{\mu+\delta+\xi_0}, 0, 0\right)$, to have [6]

$$\begin{aligned} \frac{dE}{dt} &= \frac{\beta(t)(\mu+\delta)}{\mu+\delta+\xi_0} I(t) - (\mu+\kappa)E(t) \\ \frac{dI}{dt} &= \kappa E(t) - (\mu+\gamma)I(t), \end{aligned}$$

so that the transmissibility number is

$$\begin{aligned} \overline{\mathcal{R}}_v &= \frac{\beta_0\kappa(\mu+\delta)}{(\mu+\kappa)(\mu+\gamma)(\mu+\delta+\xi_0)} + \frac{\beta_1^2}{2} Re \left[\frac{\left(\frac{\beta_0\kappa}{(\mu+\kappa)(\mu+\gamma)(\mu+\delta+\xi_0)}\right)\left(\frac{1}{(\mu+\kappa+2\pi i)(\mu+\gamma+2\pi i)}\right)}{\left(\frac{1}{(\mu+\kappa)(\mu+\gamma)}\right) - \left(\frac{1}{(\mu+\kappa+2\pi i)(\mu+\gamma+2\pi i)}\right)} \right] \\ &= \frac{\beta_0\kappa(\mu+\delta)}{(\mu+\kappa)(\mu+\gamma)(\mu+\delta+\xi_0)} \left[1 - \frac{(\mu+\kappa)(\mu+\gamma)}{4\pi^2 + (2\mu+\kappa+\gamma)^2} \frac{\beta_1^2}{2} \right]. \end{aligned} \tag{30}$$

2.4.1 Sensitivity Analysis

Sensitivity analysis is used to determine how sensitive a model is to variations in the value of the parameters of the model and to changes in the structure of the model. Here, we ascertain how sensitive a state variable is with respect to any given parameter. First, we study the sensitivity of the transmissibility number with respect to the vaccination parameter, by finding the partial derivative of $\overline{\mathcal{R}}_v$ with respect to ξ_0. This yields:

$$\begin{aligned}\frac{\partial\overline{\mathcal{R}}_v}{\partial\xi_0} &= -\left(\frac{\beta_0\kappa(\mu+\delta)}{(\mu+\kappa)(\mu+\gamma)(\mu+\delta+\xi_0)^2}\right)\left(1-\frac{(\mu+\kappa)(\mu+\gamma)}{4\pi^2+(2\mu+\kappa+\gamma)^2}\frac{\beta_1^2}{2}\right)\\ &= -\frac{\overline{\mathcal{R}}_v(\xi_0)}{\mu+\delta+\xi_0} < 0,\end{aligned}$$

since $\overline{\mathcal{R}}_v(\xi_0) > 0$, $\xi_0 \geq 0$, and the parameters μ and ξ are positive. The negative rate of change of the transmissibility number with respect to the vaccination rate, indicates that $\overline{\mathcal{R}}_v$ is decreasing with respect to the parameter ξ_0.

We now ascertain the sensitivity analysis of $I(t)$ with respect to the vaccination parameter ξ_0, by analyzing the equations:

$$\begin{aligned}\frac{\partial X}{\partial t} &= f(X(t,\theta),\theta)\\ \frac{d}{dt}\frac{\partial X}{\partial\theta} &= \frac{\partial f}{\partial X}\frac{\partial X}{\partial\theta}+\frac{\partial f}{\partial\theta},\end{aligned}$$

where $\theta = (\beta_0, \beta_1, \mu, \kappa, \gamma, \delta, \xi_0, N)$ and $X = (S, E, I, R)$. From these equations, we solve for $\frac{\partial X}{\partial\theta}$ and ascertain how sensitive, $I \in X$ is with respect to $\xi_0 \in \theta$, as depicted in the Figure 5.

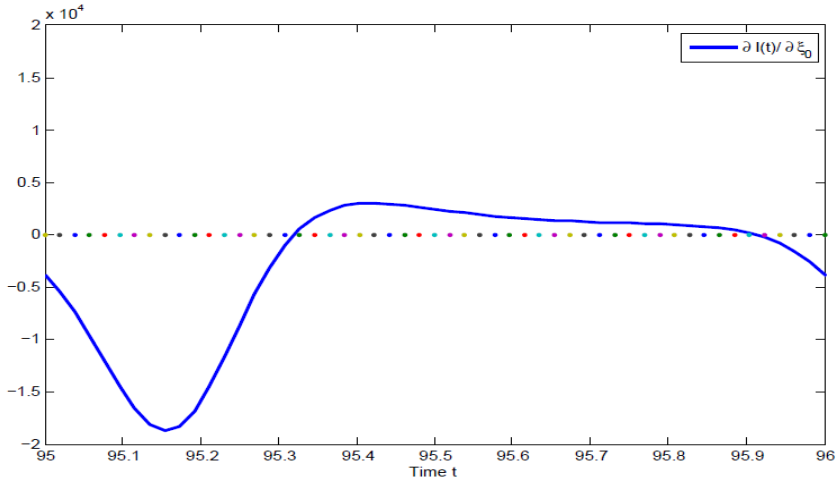

Figure 5: Sensitivity of $I(t)$ with Respect to $\xi(t)$ when $\beta_0 = 370$, $\beta_1 = 0.0283$, $\mu = 0.0133$, $\delta = 0.2$, $\kappa = 182.5$, $\gamma = 104.2857$, $\pi = 3.14$, $\xi_0 = 0.005$ and $t = 1 : \frac{1}{52} : 100$

In Figure 5, the rate of change of $I(t)$ with respect to ξ_0 is negative from time $[95, 95.3]$ and $[95.9, 96]$ years. This suggests that the population of the infectives decreases with respect to the vaccination parameter ξ_0 in these intervals.

3 NUMERICAL SIMULATIONS

Programs (or codes) were written in MATLAB to simulate the non-seasonal and seasonal models given in systems (3), (23) and (27) and results verified using detailed outputs from a number of runs. For the numerical procedure, we selected parameters values for the parameters used in systems (3), (23) and (27). We have the following interpretation for each parameter used: For the sake of numerical illustration, we chose $N = 1 \times 10^6$ humans in the population, $\mu = 0.0133$ corresponds to the death rate per year, $\gamma = 104.2857$ corresponds to the per capita recovery rate of individuals per year, $\delta = 0.2$ is the per capita rate of loss of immunity per year, and $\kappa = 182.5$ rate of infection per week. The table below summarizes the general parameter values, units used and references but, in the context of our work, we have converted these values to weekly values, since the data obtained from the Centers for Disease Control and Prevention are weekly reports of pneumonia and influenza mortality, analyzed in Chapter 4.

Table 1: Parameter Baseline Values for the Seasonal and Non-Seasonal Models

Parameters	Definition	Baseline value	Unit	Source
N	Total population size	10^6	people	–
δ^{-1}	Average duration of immunity	5	years	[28]
γ^{-1}	Mean infectious period	3.50	days	[14]
μ^{-1}	Mean life expectancy	75.00	years	[12]
κ^{-1}	Average latency period	2.00	days	[14]
β_0	Baseline level of transmission	–	years^{-1}	–
β_1	Coefficient of seasonality strength	$(0, 1)$	dimensionless	–

For the non-seasonal model with vaccination, and $\mathcal{R}_v = \frac{\beta_0\kappa(\mu+\delta)}{(\mu+\kappa)(\mu+\gamma)(\mu+\delta+\xi_0)}$, numerical simulations reveal that orbits converge to the disease-free state $(S^0, E^0, I^0, R^0) = \left(\frac{N(\mu+\delta)}{\mu+\delta+\xi}, 0, 0, \frac{N\xi_0}{\mu+\delta+\xi_0}\right)$ when $\mathcal{R}_v < 1$, as indicated in Figures 6 and 7. This confirms the local asymptotic stability result obtained qualitatively. In Figure 6, we simulated system (12) for a time span of 100 years at weekly intervals.

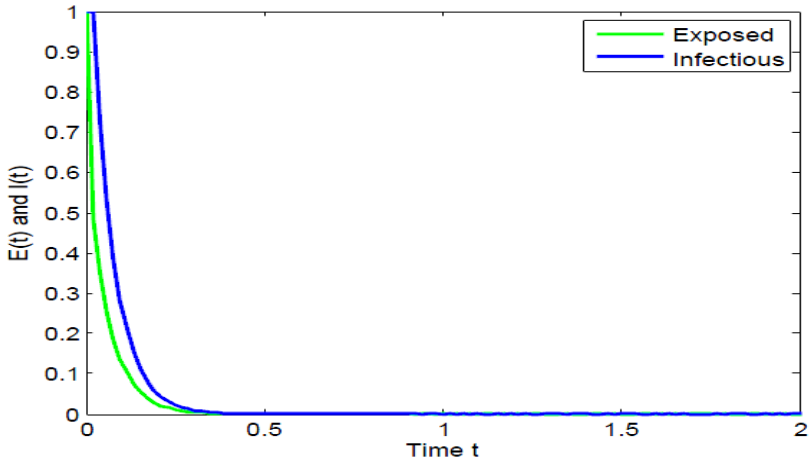

Figure 6: Infectious and Exposed Against Time for SEIRS Non-Seasonal Model when $\mathcal{R}_v < 1$, $N = 10^6$, $\beta_0 = 80$, $\mu = 0.0133$, $\delta = 0.2$, $\kappa = 182.5$, $\gamma = 104.2857$, $\xi_0 = 0.005$ and $t = 1 : \frac{1}{52} : 100$

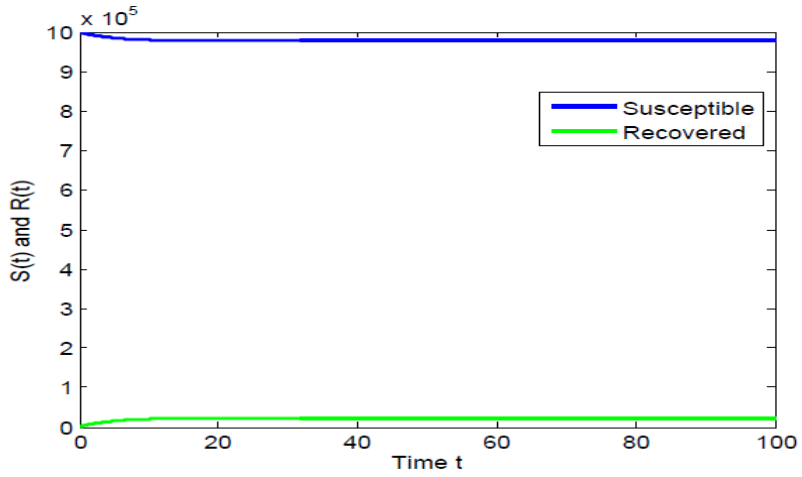

Figure 7: Stable Disease-Free Steady State Plot for Susceptible and Recovered Individuals Against Time when $\mathcal{R}_v < 1$, $N = 10^6$, $\beta_0 = 80$, $\mu = 0.0133$, $\delta = 0.2$, $\kappa = 182.5$, $\gamma = 104.2857$, $\xi_0 = 0.005$ and $t = 0 : \frac{1}{52} : 100$

When the basic reproduction number is above unity, plots of the susceptible, exposed, infectious and recovered against time indicate that the orbits converge to the endemic equilibrium as represented in Figures 8 and 9. Thus, when $\mathcal{R}_v > 1$, the disease-free state becomes unstable and there exists a non-zero endemic equilibrium which is locally asymptotically stable. Hence, the results obtained numerically are congruent to the qualitative results obtained in Theorem 2.2.

With fixed parameters defined in Figure 10, $\overline{\mathcal{R}}_v < \mathcal{R}_v < 1$. Thus, by Theorems 2.1 and 2.2, the disease-free periodic solution $(S^0, E^0, I^0, R^0) = \left(\frac{N(\mu+\delta)}{\mu+\delta+\xi_0}, 0, 0, \frac{N\xi_0}{\mu+\delta+\xi_0}\right)$ is locally asymptotically stable and the disease becomes extinct [44, 61, 62, 63]. Also, with fixed parameters defined in Figure 11, $\mathcal{R}_v > \overline{\mathcal{R}}_v > 1$. Thus, the population of the infectives proliferates and the disease persists [38].

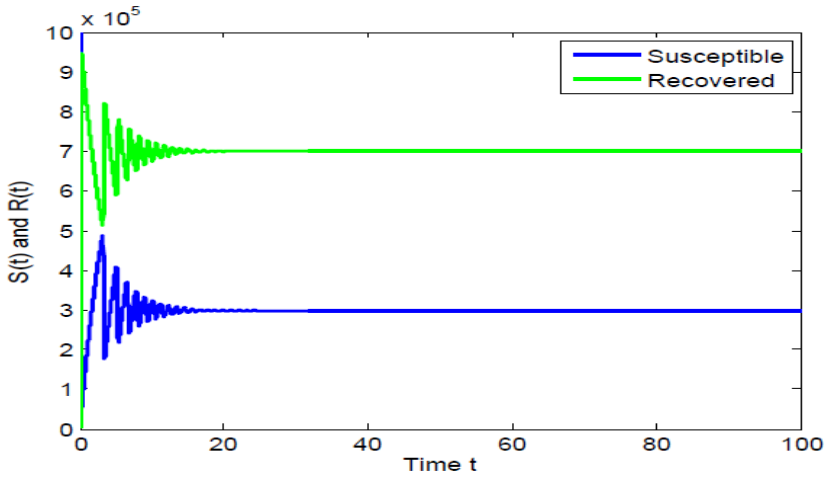

Figure 8: Susceptibles and Recovered Against Time when $\mathcal{R}_v > 1$, $N = 10^6$, $\beta_0 = 370$, $\mu = 0.0133$, $\delta = 0.2$, $\kappa = 182.5$, $\gamma = 104.2857$, $\xi_0 = 0.005$ and $t = 0 : \frac{1}{52} : 100$

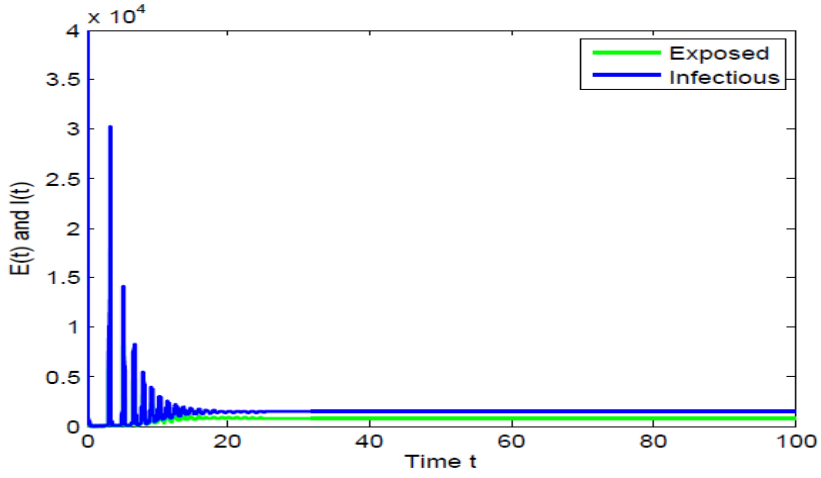

Figure 9: Exposed and Infectious Against Time when $\mathcal{R}_v < 1$, $N = 10^6$, $\beta_0 = 370$, $\mu = 0.0133$, $\delta = 0.2$, $\kappa = 182.5$, $\gamma = 104.2857$, $\xi_0 = 0.005$ and $t = 0 : \frac{1}{52} : 100$

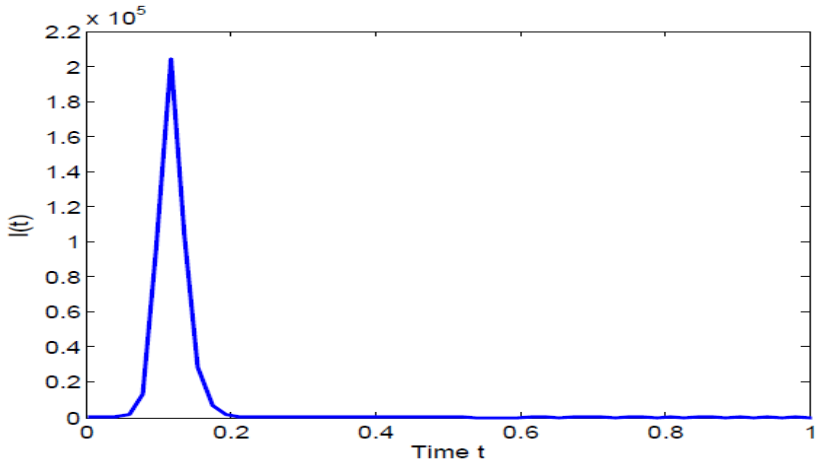

Figure 10: Infectious Individuals Against Time for SEIRS Seasonal Model when $N = 10^6$, $\beta_0 = 250$, $\beta_1 = 0.6$, $\mu = 0.0133$, $\delta = 0.2$, $\kappa = 182.5$, $\gamma = 104.2857$, $\pi = 3.14$, $\xi_0 = 0.5$, $\overline{\mathcal{R}}_v = 0.6870 < 1$, $\mathcal{R}_v = 0.7168 < 1 (\beta_1 = 0)$ and $t = 1 : \frac{1}{52} : 100$

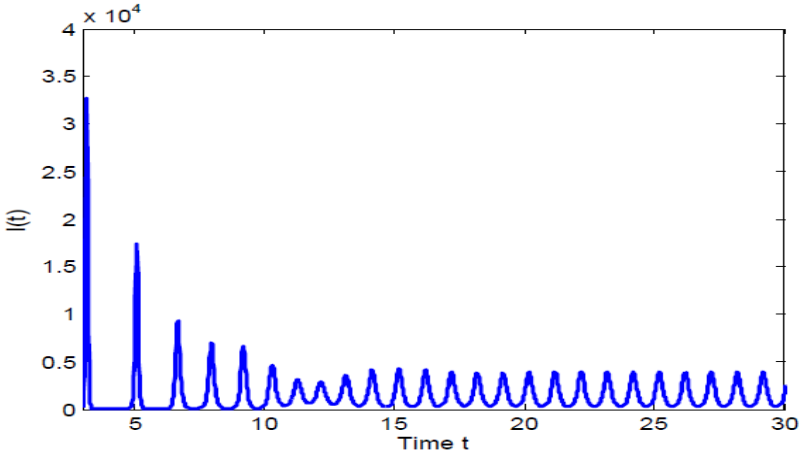

Figure 11: Infectious Individuals Against Time for SEIRS Seasonal Model when $N = 10^6$, $\beta_0 = 250$, $\beta_1 = 0.0283$, $\mu = 0.0133$, $\delta = 0.2$, $\kappa = 182.5$, $\gamma = 104.2857$, $\pi = 3.14$, $\xi_0 = 0.005$, $\overline{\mathcal{R}}_v = 2.3417 > 1$, $\mathcal{R}_v = 2.4657 > 1$ and $t = 1 : \frac{1}{52} : 100$

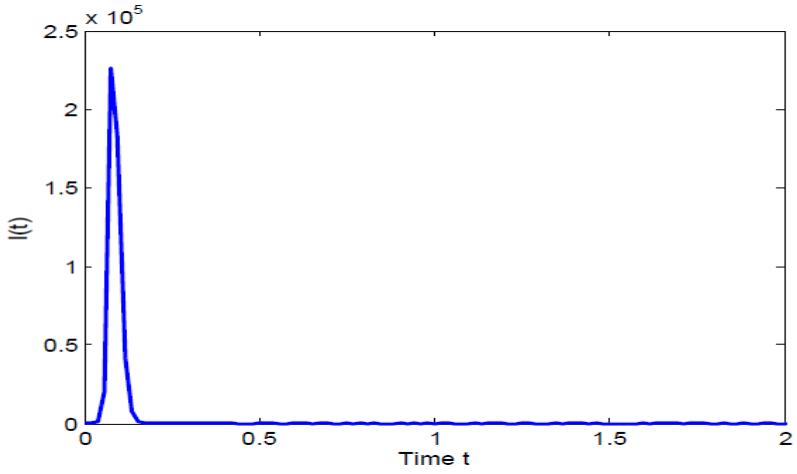

Figure 12: Infectious Individuals Against Time for SEIRS Seasonal Model when $N = 10^6$, $\beta_0 = 350$, $\beta_1 = 0.6$, $\mu = 0.0133$, $\delta = 0.2$, $\kappa = 182.5$, $\gamma = 104.2857$, $\pi = 3.14$, $\xi_0 = 0.5$, $\overline{\mathcal{R}}_v = 0.9617 < 1$, $\mathcal{R}_v = 1.0035 > 1$ and $t = 1 : \frac{1}{52} : 100$

With fixed parameters defined in Figure 12, $\overline{\mathcal{R}}_v \simeq 0.9617 < 1$. Thus, by Theorems 2.1 and 2.2, the disease-free periodic solution $(S^0, E^0, I^0, R^0) = \left(\frac{N(\mu+\delta)}{\mu+\delta+\xi_0}, 0, 0, \frac{N\xi_0}{\mu+\delta+\xi_0}\right)$ is locally asymptotically stable and the disease dies out. Moreover, if $\beta_1 = 0$, the the basic reproduction of the autonomous system $\mathcal{R}_v \simeq 1.0035 > 1$, and we would expect that the disease persists. This suggests that the eradication policy on the basis of the basic reproduction number, $\mathcal{R}_v$, of the autonomous system may overestimate the infectious risk in a scenario where the disease portrays seasonal behavior [61].

We now assume a form for the vaccination parameter $\xi(t)$, where $\xi(t)$ is nonzero during periods where the sensitivity depicted in Figure 5 is negative and zero otherwise. Thus, $\xi(t)$ is defined as a stepwise constant function of the form given in Figure 13

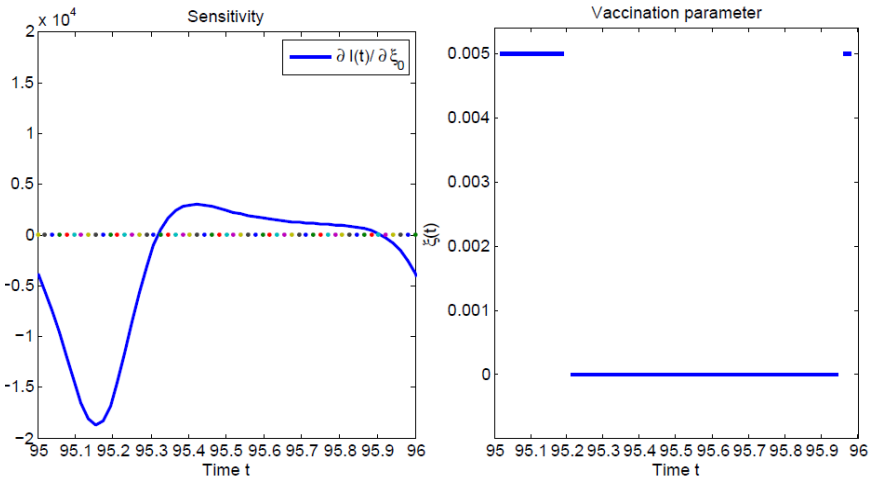

Figure 13: Plots of $\xi(t)$ and $I(t)$ with Respect to $\xi(t)$ when $\beta_0 = 370$, $\beta_1 = 0.0283$, $\mu = 0.0133$, $\delta = 0.2$, $\kappa = 182.5$, $\gamma = 104.2857$, $\pi = 3.14$, $\xi_0 = 0.005$ and $t = 1 : \frac{1}{52} : 100$

We study routine vaccination by assuming that, $\xi(t)$ takes the form

$$\xi(t) = \begin{cases} \xi_0, & t \leq \tau \\ \xi_1, & t > \tau \end{cases} \tag{31}$$

In Figure 14, the blue curve represents the population of the infectives without vaccination and the green curve represents the population of the infectious individuals when routine vaccination of the form (31) is administered. Prevalence of infection over time for a seasonal SEIRS model where the introduction of routine vaccination

at time 90 years results in a decrease in the maximum of prevalence of the infectious individuals in the population, but this decrease is unsustained.

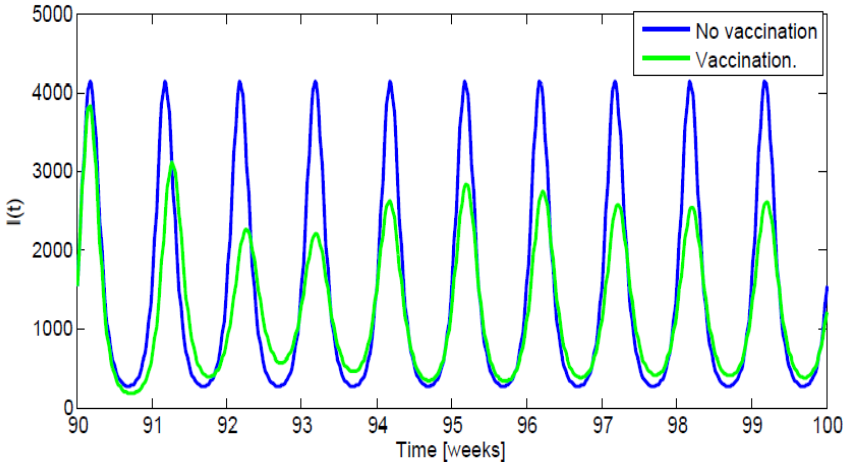

Figure 14: Routine Vaccination from $90-92$ of the form (31) when $N = 10^6$, $\beta_0 = 250$, $\beta_1 = 0.0283$, $\mu = 0.0133$, $\delta = 0.2$, $\kappa = 182.5$, $\gamma = 104.2857$, $\pi = 3.14$, $\xi_0 = 0$, $\xi_1 = 0.5$ and $t = 1 : \frac{1}{52} : 100$

Thus, we choose another form for the vaccination parameter that takes into account pulse vaccination, namely,

$$\xi(t) = \begin{cases} \xi_0, & t \leq \tau_1 \\ \xi_1, & \tau_1 < t \leq \tau_2 \\ \xi_0, & \tau_2 < t \leq \tau_3 \\ \xi_1, & \tau_3 < t \leq \tau_4 \\ \xi_0, & \tau_4 < t \leq \tau_5. \end{cases} \tag{32}$$

This yields the simulations in Figures $15 - 18$, together with a specific form of $\xi(t)$ for each figure.

$$\xi(t) = \begin{cases} \xi_0, & t \leq 90 \\ \xi_1, & 90 < t \leq 90.2 \\ \xi_0, & 90.2 < t \leq 90.9 \\ \xi_1, & 90.9 < t \leq 91 \\ \xi_0, & 91 < t \leq 92 \\ \xi_1, & 92 < t \leq 92.2 \\ \xi_0, & 92.2 < t \leq 92.9 \\ \xi_1, & 92.9 < t \leq 93 \\ \xi_0, & 93 < t \leq 100 \end{cases}$$

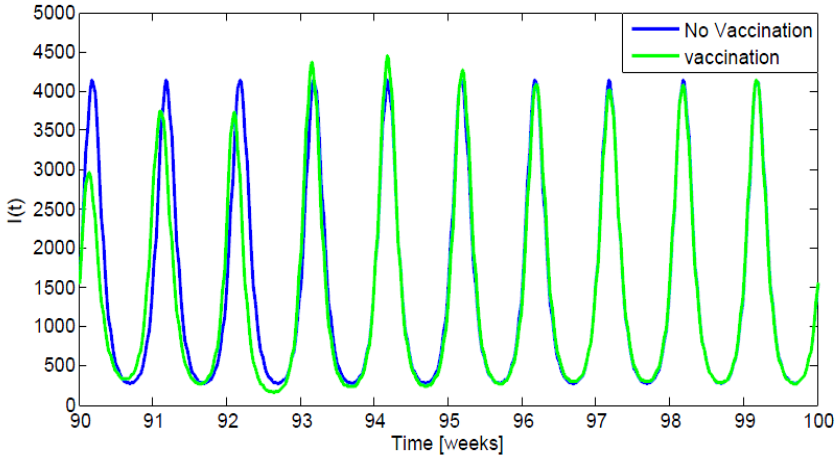

Figure 15: One Year on, One Year off, One Year on and off Onwards Pulse Vaccination from $90 - 92$ Years of the form (32) when $N = 1000000$, $\beta_0 = 250$, $\beta_1 = 0.0283$, $\mu = 0.0133$, $\delta = 0.2$, $\kappa = 182.5$, $\gamma = 104.2857$, $\pi = 3.14$, $\xi_0 = 0$, $\xi_1 = 0.5$ and $t = 1 : \frac{1}{52} : 100$

$$\xi(t) = \begin{cases} \xi_0, & t \leq 90 \\ \xi_1, & 90 < t \leq 90.2 \\ \xi_0, & 90.2 < t \leq 90.9 \\ \xi_1, & 90.9 < t \leq 91 \\ \xi_0, & 91 < t \leq 93 \\ \xi_1, & 93 < t \leq 93.2 \\ \xi_0, & 93.2 < t \leq 93.9 \\ \xi_1, & 93.9 < t \leq 94 \\ \xi_0, & 94 < t \leq 100 \end{cases}$$

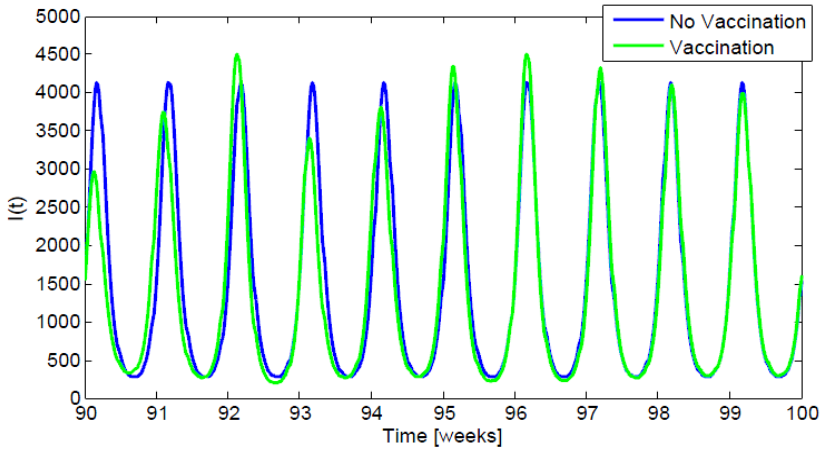

Figure 16: One Year on, Two Years off, One Year on and off Onwards Pulse Vaccination from $90 - 94$ Years when $N = 10^6$, $\beta_0 = 250$, $\beta_1 = 0.0283$, $\mu = 0.0133$, $\delta = 0.2$, $\kappa = 182.5$, $\gamma = 104.2857$, $\pi = 3.14$, $\xi_0 = 0$, $\xi_1 = 0.5$ and $t = 1 : \frac{1}{52} : 100$

$$\xi(t) = \begin{cases} \xi_0, & t \leq 90 \\ \xi_1, & 90 < t \leq 90.2 \\ \xi_0, & 90.2 < t \leq 90.9 \\ \xi_1, & 90.9 < t \leq 91 \\ \xi_0, & 91 < t \leq 92 \\ \xi_1, & 92 < t \leq 92.2 \\ \xi_0, & 92.2 < t \leq 92.9 \\ \xi_1, & 92.9 < t \leq 93 \\ \ldots, & \ldots \\ \xi_0, & 99 < t \leq 100 \end{cases}$$

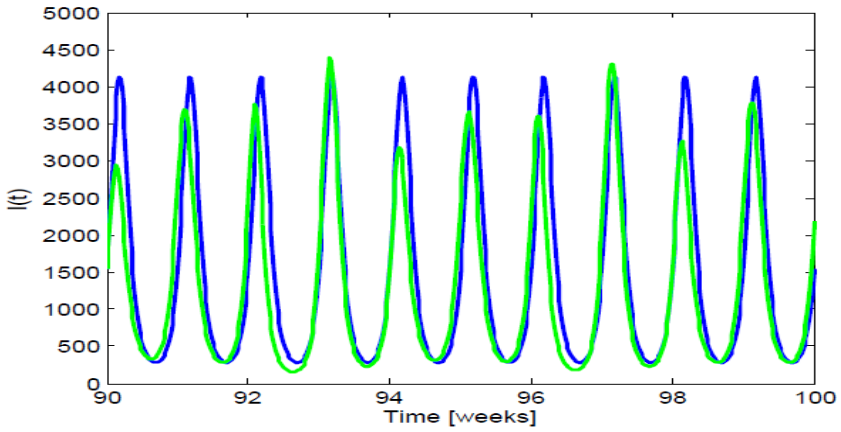

Figure 17: Every Other Year Pulse Vaccination from $90 - 100$ Years when $N = 10^6$, $\beta_0 = 250$, $\beta_1 = 0.0283$, $\mu = 0.0133$, $\delta = 0.2$, $\kappa = 182.5$, $\gamma = 104.2857$, $\pi = 3.14$, $\xi_0 = 0$, $\xi_1 = 0.5$ and $t = 1 : \frac{1}{52} : 100$

$$\xi(t) = \begin{cases} \xi_0, & t \leq 90 \\ \xi_1, & 90 < t \leq 90.2 \\ \xi_0, & 90.2 < t \leq 90.9 \\ \xi_1, & 90.9 < t \leq 91 \\ \xi_1, & 91 < t \leq 91.2 \\ \xi_0, & 91.2 < t \leq 91.9 \\ \xi_1, & 92.9 < t \leq 93 \\ \ldots, & \ldots \\ \xi_1, & 99.9 < t \leq 100 \end{cases}$$

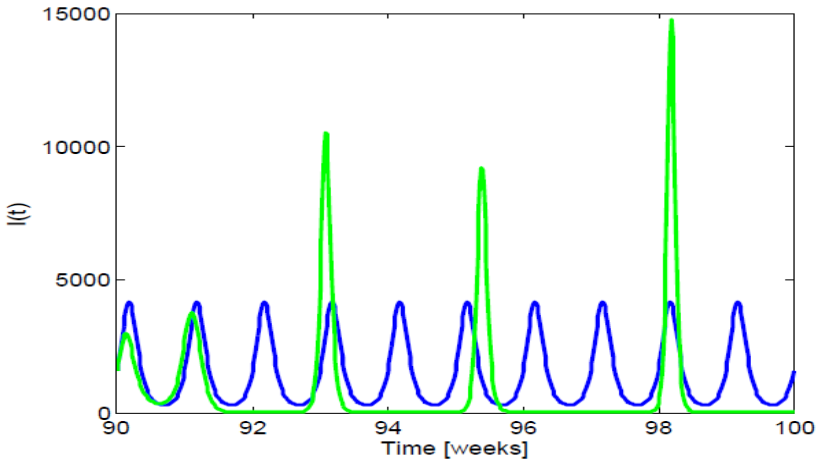

Figure 18: Every Year Pulse Vaccination from $90-100$ Years when $N = 10^6$, $\beta_0 = 250$, $\beta_1 = 0.0283$, $\mu = 0.0133$, $\delta = 0.2$, $\kappa = 182.5$, $\gamma = 104.2857$, $\pi = 3.14$, $\xi_0 = 0$, $\xi_1 = 0.5$ and $t = 1 : \frac{1}{52} : 100$

Figure 15 depicts one year on, one year off, one year on and off onwards pulse vaccination, with the administration of the vaccine during the time intervals $[90, 90.2]$, $[90.9, 91]$, $[92, 92.2]$, and $[92.9, 93]$. This leads to a decrease in the maximum of prevalence of the infectives at time $90 - 93$ years and the maximum peaks above the maximum for the unvaccinated infectives at time $93 - 95$ years. This may be ac-

counted for from the fact that, once the vaccine is administered, the infective class shrinks and other classes stretch, since the total population is constant, so that once the epidemic hits, it has an adverse effect on the population of the infectives. With a pulse vaccination strategy analogous to Figure 15, but with one year on, two years off, one year on and off onwards, the maximum of prevalence of the infectives is lowered upon the introduction of the vaccine at times $t = 90$ years, which increases in the interval $[91, 92]$ and peaks in $[92, 93]$ as depicted in Figure 16. The trend in the maximum of prevalence is repeated in the interval $[93, 95]$, but with an adverse effect on the population of the infectious individuals during the subsequent years. Finally, the introduction of annual pulse vaccination from time $t = 90$ years to $t = 100$ years results in the transition from annual epidemics to biennial epidemics in the interval $[90, 96]$ years and triennial epidemics in the time interval $[96, 98]$ years, which is a typical artifact of the seasonal model.

Finally, we propose the following form for the parameter $\xi(t)$ that takes into consideration an increase in the coverage of the vaccine:

$$\xi(t) = \begin{cases} \xi_0, & t \leq \tau_1 \\ \xi_1, & \tau_1 < t \leq \tau_2 \\ \xi_0, & \tau_2 < t \leq \tau_3 \\ \xi_1, & \tau_3 < t \leq \tau_4 \\ \xi_2, & \tau_4 < t \leq \tau_5 \\ \xi_0, & \tau_5 < t \leq \tau_6 \\ \xi_2, & \tau_6 < t \leq \tau_7 \\ \xi_3, & \tau_7 < t \leq \tau_8 \\ \xi_4, & \tau_8 < t \leq \tau_9 \\ ..., & ..., \end{cases} \tag{33}$$

where $\xi_0 < \xi_1 < \xi_2 < \xi_3 < \xi_4$.

For the seasonal model with pulse vaccination in which there is a gradual increase in

the coverage of vaccination of the form (33), we obtain the simulations depicted in Figures 19 and 20, together with specific forms of $\xi(t)$.

$$\xi(t) = \begin{cases} \xi_0, & t \leq 90 \\ \xi_1, & 90 < t \leq 90.2 \\ \xi_0, & 90.2 < t \leq 90.9 \\ \xi_1, & 90.9 < t \leq 91 \\ \xi_2, & 91 < t \leq 91.2 \\ \xi_0, & 91.2 < t \leq 91.9 \\ \xi_2, & 91.9 < t \leq 92 \\ \xi_3, & 92 < t \leq 92.2 \\ \xi_0, & 92.2 < t \leq 92.9 \\ \xi_3, & 92.9 < t \leq 93, \end{cases}$$

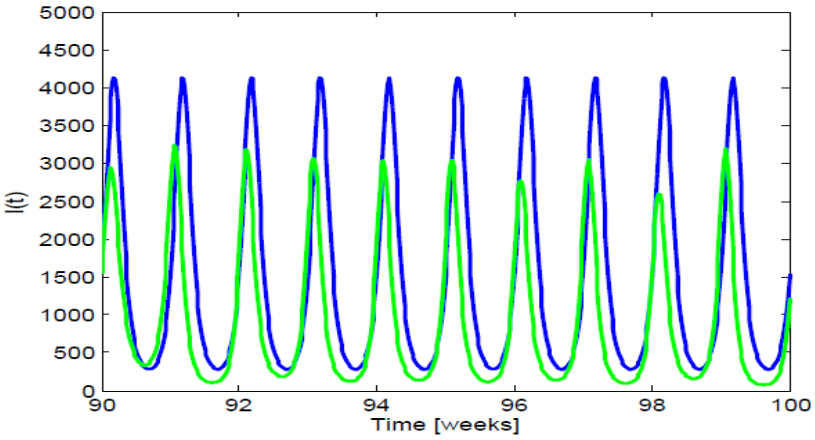

Figure 19: Every Year Pulse Vaccination from $90-100$ Years when $N = 10^6$, $\beta_0 = 250$, $\beta_1 = 0.0283$, $\mu = 0.0133$, $\delta = 0.2$, $\kappa = 182.5$, $\gamma = 104.2857$, $\pi = 3.14$, $\xi_0 = 0$, $\xi_1 = 0.5$, $\xi_2 = 0.7$, $\xi_3 = 0.75$, $\xi_4 = 0.8$, $\xi_5 = 0.85$, $\xi_6 = 0.9$, $\xi_7 = 0.91$, $\xi_8 = 0.92$, $\xi_9 = 0.93$, $\xi_{10} = 0.95$ and $t = 1 : \frac{1}{52} : 100$

$$\xi(t) = \begin{cases} \xi_0, & t \leq 90 \\ \xi_1, & 90 < t \leq 90.2 \\ \xi_0, & 90.2 < t \leq 90.9 \\ \xi_1, & 90.9 < t \leq 91 \\ \xi_2, & 91 < t \leq 91.2 \\ \xi_0, & 91.2 < t \leq 91.9 \\ \xi_2, & 91.9 < t \leq 92 \\ \xi_3, & 92 < t \leq 100, \end{cases}$$

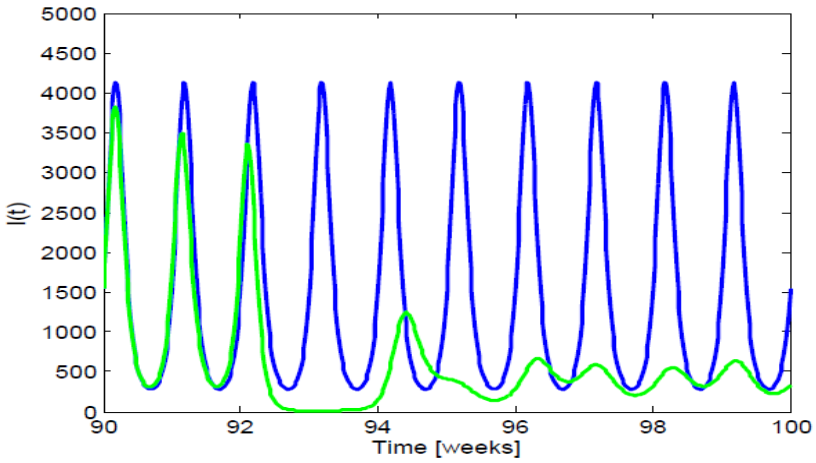

Figure 20: Every Year Pulse Vaccination from $90-100$ Years when $N = 10^6$, $\beta_0 = 250$, $\beta_1 = 0.0283$, $\mu = 0.0133$, $\delta = 0.2$, $\kappa = 182.5$, $\gamma = 104.2857$, $\pi = 3.14$, $\xi_0 = 0$, $\xi_1 = 0.1$, $\xi_2 = 0.2$, $\xi_3 = 0.3$, $\xi_4 = 0.4$ and $t = 1 : \frac{1}{52} : 100$

In Figure 19, we have articulated annual pulse vaccination from time $t = 90$ years to $t = 100$ years with an increasing coverage of the vaccine. The maxima and minima of prevalence of the infectives is lowered to an order of magnitude, and we reckon this an articulate strategy for controlling the epidemic. For a vaccination strategy that articulates an increasing vaccine coverage from $90 - 92$ years, and a constant vaccine coverage from $92 - 100$ years, we notice an appreciable decrease in the maximum of

prevalence of the infectives as depicted in Figure 20.

4 TIME SERIES ANALYSIS OF SEASONAL DATA

The seasonal data we present in this chapter are final totals of weekly mortality data of influenza and pneumonia in the United States from 1993-2010. These statistics are collected and compiled from reports sent by state health departments and territories to the National Notifiable Diseases Surveillance System (N.N.D.S.S.), which is operated by the Centers for Disease Control and Prevention (C.D.C.) in collaboration with the Council of State and Territorial Epidemiologists (C.S.T.E.) [13].

4.1 Plots, Trends, Seasonal Variations, and Periodogram

The time series of seasonal data are analyzed to understand the past and predict the future, enabling epidemiologists to make proper decisions on the variation of seasonal infections [16]. The time series data we analyze in this chapter consists of monthly observations of the morbidity and mortality weekly report of pneumonia and influenza obtained from the Centers for Disease Control and prevention (C.D.C.) from 1993-2010 [13]. In this chapter, we explore the use of graphical methods for the purpose of better understanding the underlying variation within and between time series data. One of the most important steps in a preliminary time series analysis is to plot the data. Thus, a plot of the mortality data of pneumonia and influenza against time is displayed in the Figure 21.

Figure 21 depicts mortality trends (a systematic change in time series that does not appear to be periodic) and seasonal variations (a repeating pattern within each year) for pneumonia and influenza from 1993-2010. We notice that there is a high

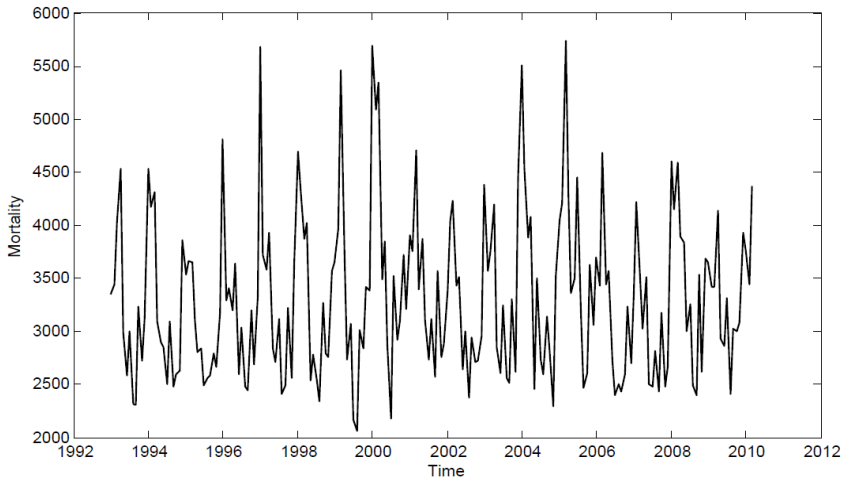

Figure 21: Seasonal Data of Pneumonia and Influenza

mortality for pneumonia and influenza during the months of December-February and low mortality from May-August. This may be accounted for from the fact that, from December-February in the United States, the atmospheric temperature is at its minimum and thus serves as an ideal breeding ground for multiplication of the parasite [9].

A useful tool for describing the time series data set above is by means of a periodogram, where the basic idea is that sinusoids of low frequency are smooth in appearance whereas sinusoids of high frequency are very wiggy [57]. Figure 22 portrays a strong sinusoidal signal for a frequency of 12.1176470588235, for example, as evident by the peak in the periodogram at this frequency.

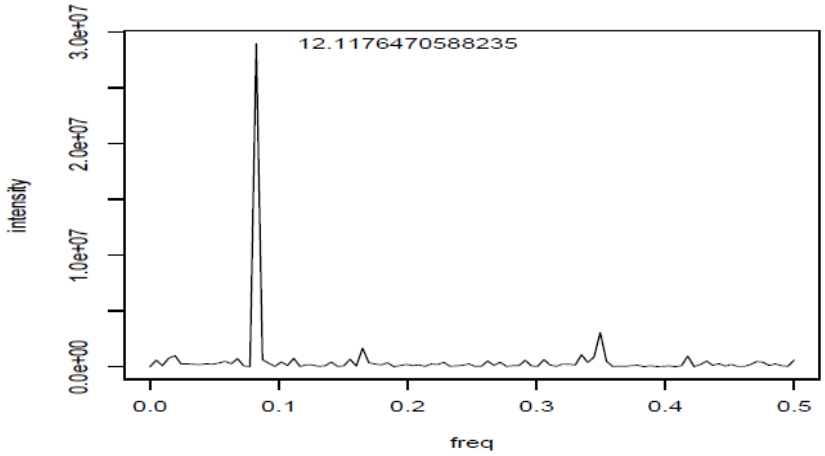

Figure 22: Periodogram of Seasonal Data of Pneumonia and Influenza

4.2 Decomposition

A common approach to time series is to consider them as a mixture of several components and decompose the data into trend, seasonality, and an irregular or random effect. It is of paramount importance to identify the trend and seasonal components, and deplete them from the time series when modeling relations between time series. When this is not done, highly seasonal series can appear to be related purely because of their seasonality rather than because of any real relationship. Time series decomposition methods allow an assessment of the strength of the seasonal component in each of the mortality variables. After identification, the seasonal component is removed and the resultant seasonally adjusted series is used in subsequent analysis. Thus, extracting the seasonal component allows a clearer picture of other characteristics of the data [9].

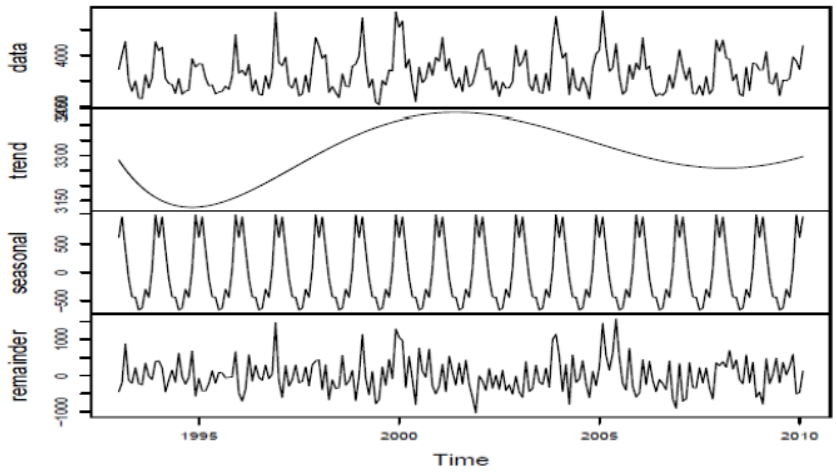

Figure 23: Decomposition of Seasonal Data of Pneumonia and Influenza

For an additive decomposition approach, we assume that

$$Y_t = T_t + S_t + R_t,$$

where Y_t denotes the time series of interest (or observed series), T_t denotes the trend component, S_t denotes the seasonal component and R_t denotes the remainder or irregular component. The seasonally adjusted series, Y_t^* is computed simply by subtracting the estimated seasonal component, S_t^*, from the original series [9, 16], which yields:

$$Y_t^* = Y_t - S_t^*.$$

A seasonal-trend decomposition consists of a sequence of applications of the loess smoother to provide robust estimates of the components T_t, S_t and R_t from Y_t. The Seasonal-Trend decomposition method involves an iterative algorithm to progressively refine and improve estimates of trend and seasonal components [9]. With this, we construct a decomposition plot, given in Figure 24, which normally consists of four

panels: the original series, the trend component, the seasonal component and the irregular (or random) component. The panels are arranged vertically so that time is a common horizontal axis for all panels. The trend component consists of the underlying long-term aperiodic [9] rises and/or falls in the level of the series over time. The seasonal component is a pattern that is recurrent over time and the irregular component is the remaining pattern in the series not attributed to trend or seasonality. Both trend and seasonality are potential confounding variables in any analysis, so their identification and removal are vital [9].

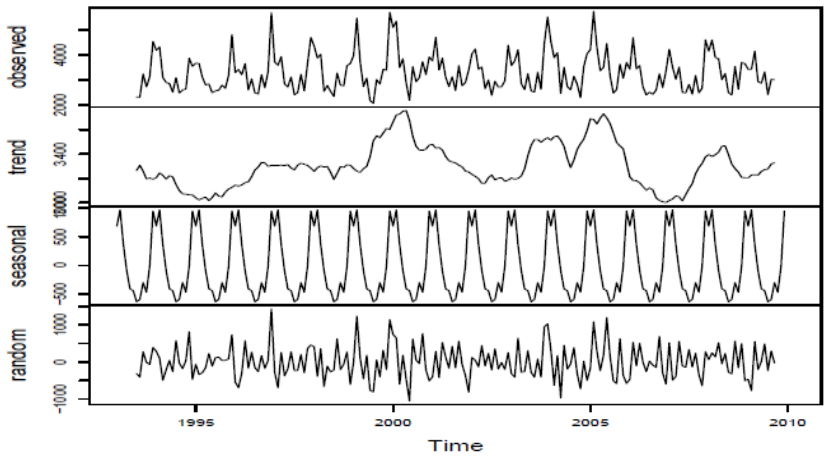

Figure 24: Additive Decomposition of Seasonal Data of Pneumonia and Influenza

The seasonal effect and irregular components are the same for a general decomposition and the additive decomposition approach but the trend for the general decomposition is non informative as it is represented by a polynomial, given in the second panel of Figure 23. In the additive decomposition, the mortality trend is high within the months of December and January in 2000, 2004, 2005 and 2009, approximately.

If the seasonal effect tends to increase as the trend increases, a multiplicative model may be more appropriate [16], where we have

$$Y_t = T_t S_t + R_t.$$

This approach leads to Figure 25:

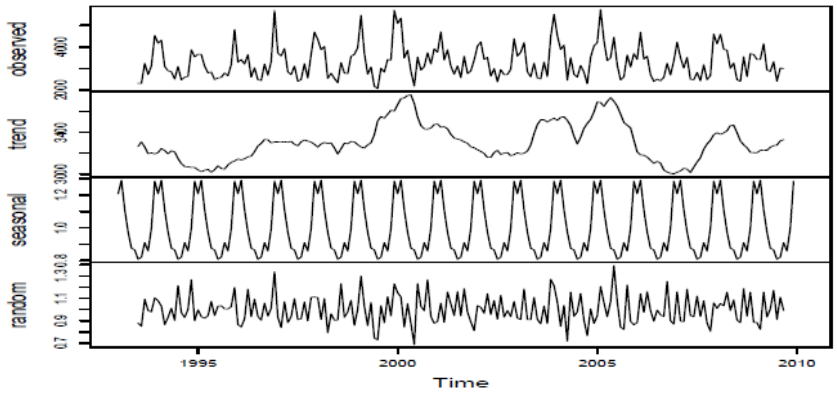

Figure 25: Multiplicative Decomposition of Seasonal Data of Pneumonia and Influenza

There is no visual difference in the trend and seasonal components of the additive and multiplicative decomposition models. So, we estimate the trend $T(t)$ at time t, by calculating a moving average centered at $Y(t)$ from the formula [16]

$$\hat{Y_t} = \frac{\frac{1}{2}Y_{t-6} + Y_{t-5} + ... + Y_{t+5} + Y_{t+6}}{12},$$

where $t = 7, 6, ..., n-6$. A moving average is an average of a specified number of time series values around each value in the time series, with the exception of the first few and last few terms. The length of the moving average is chosen to average twelve consecutive months, but there is a slight snag, since this average corresponds to a

time $t = 6.5$, between June and July as we start at January ($t = 1$) and average up to December ($t = 12$). The estimation of seasonal effects requires moving averages at integer times, which is achieved by averaging the average of January ($t = 1$) up to December ($t = 12$) and the average of February ($t = 2$) up to January ($t = 13$) [16]. Since in Figure 25, the seasonal effect does not increase as the trends increases, the multiplicative decomposition model is not suitable for the decomposition.

A number of time series decomposition methods are available, one of which is the classical decomposition. Classical decomposition is a relatively simple method, but has several disadvantages, including bias problems near the ends of the series and an inability to allow a smoothly varying seasonal component [9]. To overcome these difficulties we adopt the Seasonal-Trend decomposition procedure based on loess smoothing to have the Loess plot for the seasonal data of pneumonia and influenza from 1993-2010 [13] given in Figure 26 [57]. In Figure 26, we have separated the smooth curve estimated in Figure 21 into two components due to trend and seasonality, so that the seasonal component in the third panel of the Loess plot captures the drop in summer and increase in winter of pneumonia and influenza mortality (as a result of high and low temperatures, respectively). The bottom panel displays what remains when the trend and seasonal components are removed from the mortality data. This gives a way of determining unusual periods of the year without confusing which occurs as a result of seasonality. Also, the trend increases with decreasing seasonal effect. Thus, the Loess smoother is not apt for the decomposition.

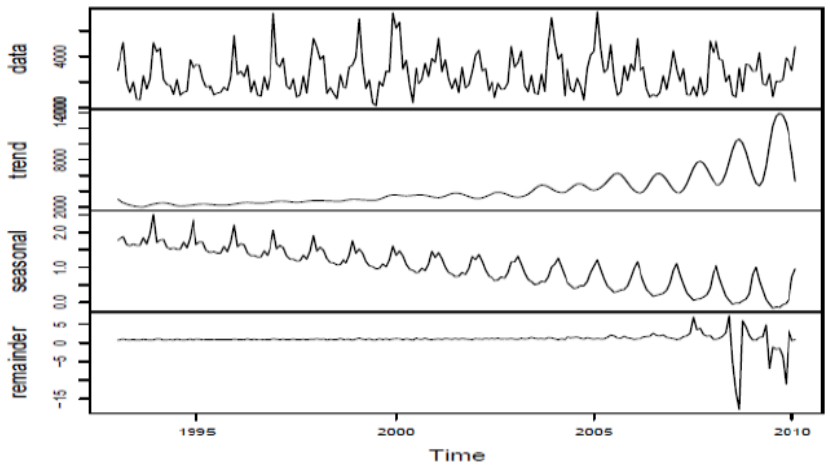

Figure 26: Loess Plot of Seasonal Data of Pneumonia and Influenza Mortality

4.3 Correlation

We deseasonalize the time series and remove the trends since these trends and seasonal effects have been identified. This leaves the random component, which is not necessarily well modeled by in dependent random variables, in which consecutive random variables may be correlated [16].

The following definitions will be useful: the expected value, E, commonly called expectation of a variable X or a function of a variable, is its mean value in the population, given by $\mu = E(X) = \sum xP(X = x)$, and $E(X - \mu)^2$ is the mean of the squared deviations, commonly called the variance. The square root of the variance is known as the standard deviation. If there are two variables X and Y, the variance may be generalized to the covariance, σ_{XY}, defined by

$$\sigma_{XY} = E[(X - \mu_X)(Y - \mu_Y)],$$

which measures a linear association between the variables. For n data values, the covariance becomes:

$$Cov(X,Y) = \frac{1}{n-1}\sum E[(X_i - \overline{X})(Y_i - \overline{Y})],$$

with the population and sample correlation defined by

$$\rho(X,Y) = \frac{\sigma(X,Y)}{\sigma_X \sigma_Y},$$

and $Cor(X,Y) = \frac{Cov(X,Y)}{sd(X)sd(Y)}$. Autocorrelation is the correlation of a variable with itself at different times, x_i and x_{i+k}. A correlogram or autocorrelation plot is a plot of the sample autocorrelations against lags and is useful for ascertaining the randomness in a data set, where a lag is the number of time steps between the variable. If the data set is random, then such correlogram should be near zero for all time lags, else one or more of the autocorrelations will be significantly non-zero. A time series model is second-order-stationary if the correlation between variables depend only on the number of time steps separating them. If the time series is second-order-stationary, we define the autocovariance function by

$$\gamma_k = E[(x_t - \mu)(x_{t+k} - \mu)].$$

The ACF or lag k autocorrelation function is defined by

$$\rho_k = \frac{\gamma_k}{\sigma^2}.$$

In Figure 27, the ACF (which returns the correlogram or sets its argument to obtain autocovariance function) of the residuals are not strictly iid random normal variables, but have some seasonal effect on it. The correlation at lags 0.0, 0.1 and

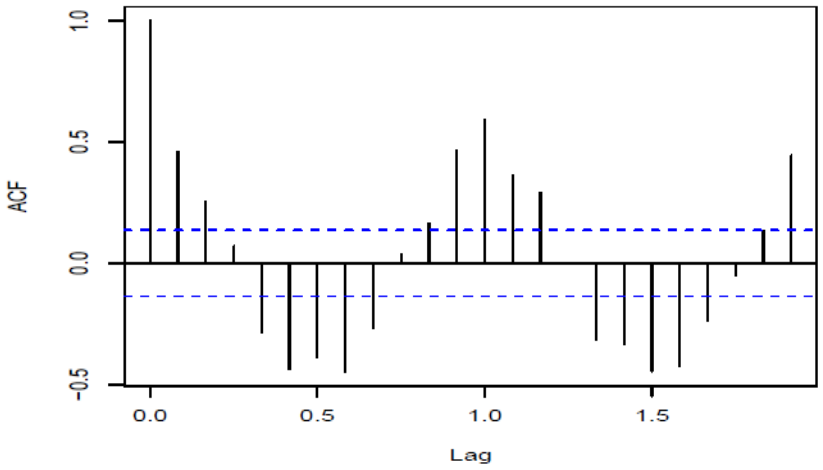

Figure 27: Correlogram of Seasonal Data of Pneumonia and Influenza Mortality

0.2 are significant, indicating the residuals are not independent, but related to the previous residual. The correlations at lags 0.3, 0.4, 0.5, 0.6, 0.7 are significant and negative, which are probably caused by seasonal change.

4.4 Forecasting

In forecasting the mortality of pneumonia and influenza, the following definition shall be useful: The sum of squared one-step-ahead prediction errors, SS1PE, is

$$SS1PE = \sum_{t=2}^{n} e_t^2,$$

where the one-step-ahead prediction errors, e_t, are given by

$$e_t = x_t - \hat{x}_{t|t-1}.$$

Time-series can be represented as a curve that evolves over time. Forecasting the time-series entails an extension of historical values into the future where the

measurements are not available. In the exploration of time series of mortality data, we use a following multiplicative Holt-Winter's model.

$$\begin{aligned} a_n &= \alpha_1 \left(\frac{x_n}{s_{n-p}} \right) + (1 - \alpha_1)(a_{n-1} + b_{n-1}) \\ b_n &= \beta_1 (a_n - a_{n-1}) + (1 - \beta_1) b_{n-1} \\ s_n &= \gamma_1 \left(\frac{x_n}{a_n} \right) + (1 - \gamma_1) s_{n-p}, \end{aligned}$$

where a_n, b_n and s_n are the estimated level, slope and seasonal effect at time n respectively, x_n is an observation and α_1, β_1 and γ_1 are smoothing parameters. For the multiplicative Holt-Winter's model with $\alpha = \beta = \gamma = 0.2$ [16], a plot of the filtered values along with the observed data is given in Figure 28, and the sum of squared one-step-ahead prediction errors, SS1PE, is 557.4331.

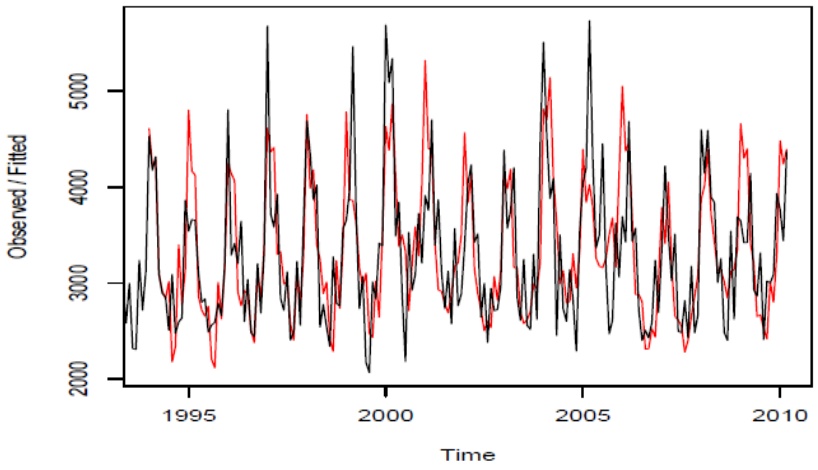

Figure 28: Filtered and Observed Multiplicative Holt-Winter's Fit for Seasonal Data of Pneumonia and Influenza with Specified Smoothing Parameter Values

Using the R Holt-Winter function without giving specific parameters, results in the optimized Holt-Winter model have a slightly better fit than the previous one, and SS1PE reduced to SS1PE= 517.4873. Since fit in Figure 29 is better and the SS1PE is smaller for the optimized Holt-Winter, we use R Holt-Winter function in our subsequent analysis.

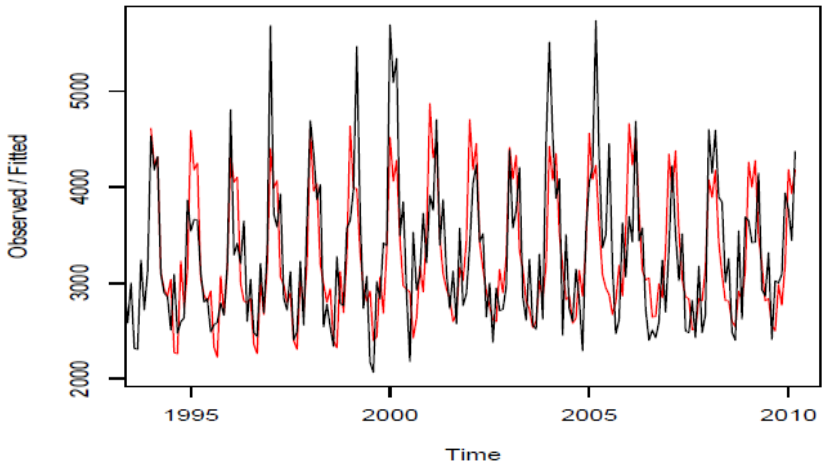

Figure 29: Filtered and Observed Multiplicative Holt-Winter's Fit for Seasonal Data of Pneumonia and Influenza

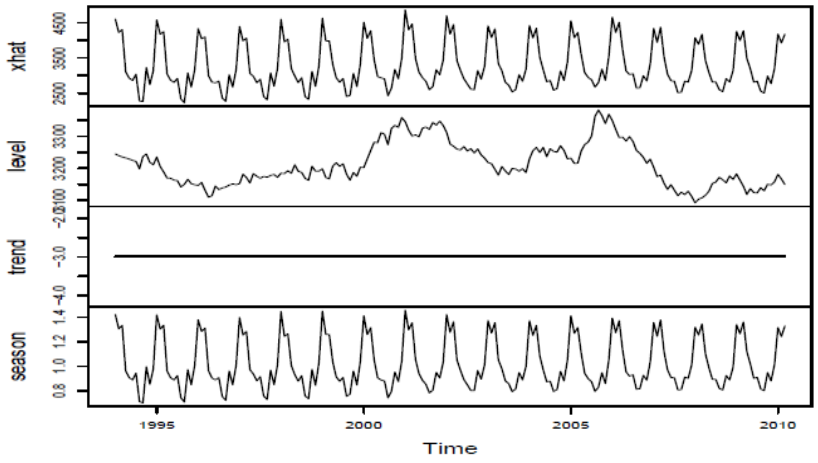

Figure 30: Multiplicative Holt-Winter's Decomposition of Seasonal Data of Pneumonia and Influenza

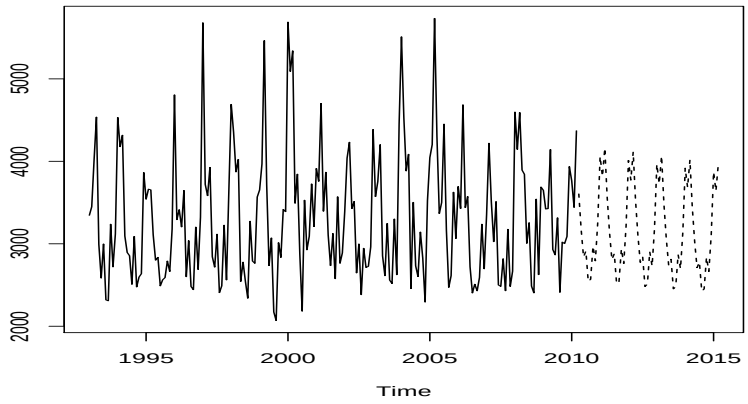

Figure 31: Multiplicative Holt-Winter's Forecasts for Seasonal Data of Pneumonia and Influenza

Figure 30 depicts a multiplicative Holt-Winter decomposition method with SS1PE value of 517.4873 and parameter values of $\alpha = 0.03585968$, $\beta = 0$, and $\gamma = 0.1269991$. The value of $\beta = 0$ is an indication that there is no trend as evident by the horizontal line in the third panel of Figure 30.

The forecast in Figure 31 is true only when the trend of the pneumonia and influenza mortality continues as the previous years (that is, no measured deaths occur that could change the mortality rate from 2010-2015). Forecasts cannot be used for a long time ahead, since errors will accumulate and may perturb the trend. The five-year forecast predicts a decrease in the mortality rate as illustrated in Figure 30.

An additive Holt-Winter's model is defined by the follwing equations:

$$\begin{aligned} a_t &= \alpha_1(x_t - s_{t-p}) + (1-\alpha_1)(a_{t-1} + b_{t-1}) \\ b_t &= \beta_1(a_t - a_{t-1}) + (1-\beta_1)b_{t-1} \\ s_t &= \gamma_1(x_t - a_t) + (1-\gamma_1)s_{t-p}, \end{aligned}$$

where a_t, b_t and s_t are the estimated level, slope and seasonal effect at time t respectively, and α_1, β_1 and γ_1 are smoothing parameters. The additive Holt-Winter's decomposition is depicted in Figure 32. We notice that the mortality data has an obvious trend and strong seasonal effect, and the trend+seasonal plot in Figure 33 has a better fit for the additive model. So, the additive Holt-Winter's model is most appropriate for decomposition and we let the Holt-Winter's function ascertain the optimal parameters automatically. The result shows that $SS1PE = 515.0608$, $\alpha = 0.05679602$, $\beta = 0.00148517$, and $\gamma = 0.1277516$. Since the SS1PE values is smaller for the additive Holt-Winter's model than for the multiplicative model, and the parameters α, β and γ are all non-zeroes, we conclude that this method is model suitable for our decomposition.

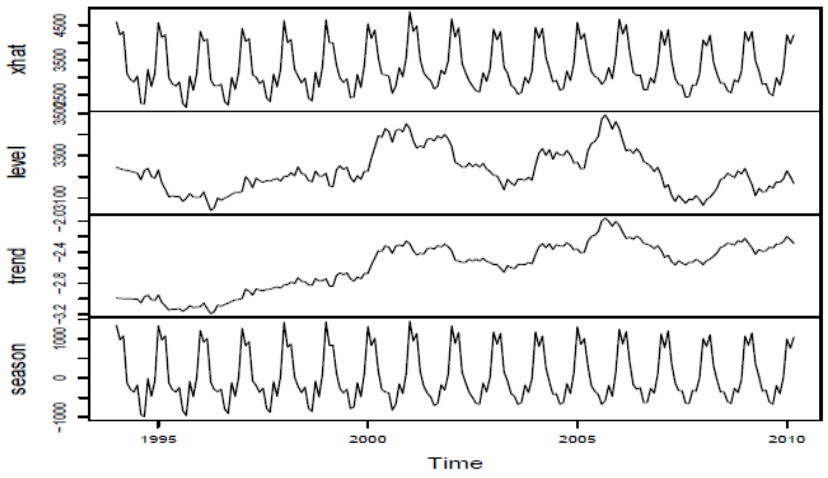

Figure 32: Additive Holt-Winter's Decomposition of Seasonal Data of Pneumonia and Influenza

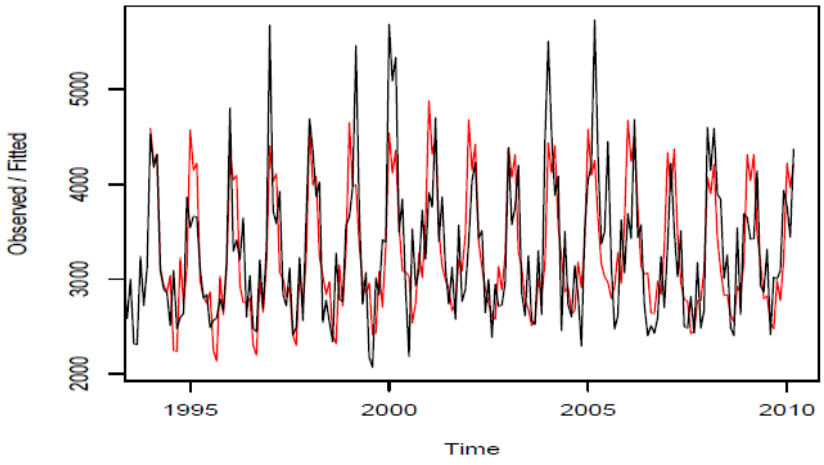

Figure 33: Filtered and Observed Additive Holt-Winter's Fit for Seasonal Data of Pneumonia and Influenza

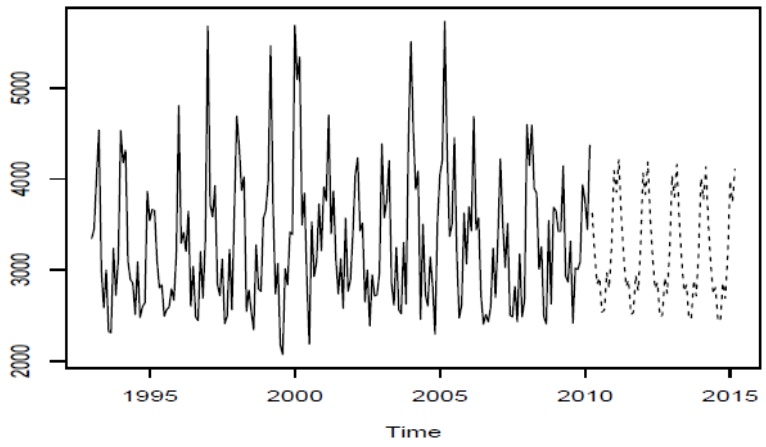

Figure 34: Additive Holt-Winter's Forecasts for Seasonal Data of Pneumonia and Influenza

The additive Holt-Winter's forecast in Figure 34 predicts a decrease in mortality of pneumonia and influenza in the United States from $2011 - 2015$. The forecast was based on the decrease in mortality from $2005 - 2010$.

5 CONCLUSION

We began the study by making some assumptions underlying a susceptible-exposed-infectious-recovered-susceptible (SEIRS) model, and proceeded to derive an SEIRS model for the dynamics and transmission of seasonal infections in a constant population. Furthermore, we assumed forms for the transmission rate and derived non-seasonal (constant transmission rate) and seasonal (sinusoidal transmission rate) models. For the non-seasonal model, we determined the basic reproduction number $\mathcal{R}_0$, using the *next generation operator approach*, and examined conditions for the existence of realistic steady states. We proved, by using the principle of linearized stability and Routh Hurwitz conditions [47], that the stability of the disease-free and endemic equilibria are controlled by one threshold parameter; namely, the basic reproduction ratio, $\mathcal{R}_0$. We showed that the disease-free equilibrium always exists and is locally and asymptotically stable if $\mathcal{R}_0 < 1$ and unstable if $\mathcal{R}_0 > 1$. If $\mathcal{R}_0 > 1$, we showed that there exists an endemic equilibrium which is locally and asymptotically stable. Deriving and examining a non-seasonal SEIRS model with vaccination, we obtained analogous results. We showed that the disease-free equilibrium always exists and is locally and asymptotically stable if $\mathcal{R}_v < 1$ and unstable if $\mathcal{R}_v > 1$, where $\mathcal{R}_v$ is the basic reproduction number of the non-seasonal model with vaccination. If $\mathcal{R}_v > 1$, we showed that there exists an endemic equilibrium which is locally and asymptotically stable. Numerical simulations for the SEIRS non-seasonal model with vaccination indicate that orbits for the exposed and infectious individuals decay whereas the orbits for the susceptible and recovered or temporary immune individuals are sustained whenever $\mathcal{R}_v < 1$. When $\mathcal{R}_v > 1$, orbits for the susceptible,

exposed, infectious and recovered individuals are sustained after a transient state, and hence the disease persists in the population. These numerical results are congruent to qualitative results obtained.

For the seasonal model with and without vaccination, we determined the transmissibility numbers, $\mathcal{R}_v$ and $\overline{\mathcal{R}}_v$, respectively, through the spectral radius of a linear integral operator on a space of periodic functions. We showed with numerical solutions that when $\overline{\mathcal{R}}_v < \mathcal{R}_v < 1$, the disease-free periodic solution is locally asymptotically stable and hence, the disease dies out. Moreover, when $\mathcal{R}_v > \overline{\mathcal{R}}_v > 1$, the infectives proliferate in the population and hence, the disease persists. Numerical solutions indicate that when $\overline{\mathcal{R}}_v < 1 < \mathcal{R}_v$, the infectives become extinct. This suggests that the eradication policy on the basis of the basic reproduction number, $\mathcal{R}_v$, of the autonomous system may overestimate the infectious risk in a scenario where the disease portrays seasonal behavior [61].

We carried out numerical experiments on the seasonal model with vaccination by assuming the vaccination parameter is a stepwise defined function which was motivated by a sensitivity analysis. This analysis revealed that during certain intervals within one period, an increase in the vaccination parameter would lead to a decrease in the population of the infectious individuals. We defined the time dependent vaccination parameter so that routine and pulse vaccinations are incorporated into our model. The prevalence of infection over time after the introduction of routine vaccination at time 90 years, results in an unsustained decrease in the maximum of prevalence of the infectious individuals. Annual pulse vaccination from time $t = 90$ to $t = 100$ years, results in the transition from annual to biennial epidemics during

certain periods and triennial epidemics during others. On the other hand, we incorporated pulse vaccination with an increasing coverage of the vaccine that depicts a decrease in the extrema of prevalence of the infectious individuals by an order of magnitude.

We used some graphical methods for time series analysis of seasonal data of pneumonia and influenza. We applied the time series plot of mortality data, periodogram, and decomposition plots to enable a visual assessment of long-term trend, seasonality and irregularity in time series data of pneumonia and influenza for 1993-2010 in the United States. We carried out an additive and a multiplicative Holt-Winter's decomposition of mortality data of pneumonia and influenza and noticed that the additive approach was apt for our data since it had a smaller sum of squared one-step-ahead prediction error (SS1PE). A forecasting procedure based on the additive Holt-Winter's model predicts a decrease in the peaks of mortality from 2011-2015 in the United States.

Some aspects of the model such as the analysis of the seasonal model with vaccination for $\overline{\mathcal{R}}_v < 1 < \mathcal{R}_v$, and the relationship between the seasonal model and seasonal data have not been examined closely. These and others are subjects for future work.

BIBLIOGRAPHY

[1] R. M. Anderson, ED., Population Dynamics of Infectious Diseases, Chapman and Hall, London, (1982).

[2] R. M. Anderson, R. M. May. EDs., Population Biology of Infectious Diseases, Springer Verlag, Berlin, Heidelberg, New York, (1982).

[3] R. M. Anderson, R. M. May. EDs., Vaccination against rubella and measles: Quantitative investigations of different policies, *J. Hyg. Camb.* **90** (1983), 259-325.

[4] R. M. Anderson, R. M. May. EDs., Infectious Diseases of Humans: Dynamics and Control, Oxford University Press, Oxford, UK, (1991).

[5] N. Bacaer, Approximation of the basic reproduction number $\mathcal{R}_0$ for vector-Borne viseases with a periodic vector population, *Bull. Math. Biol.* **69** (2007), 1067-1091.

[6] N. Bacaer, X. Abdurahman, Resonance of the epidemic threshold in a periodic environment, *J. Math. Biol.* **57** (2008), 649-673.

[7] C. Bauch, J. D. Earn, Interepidemic intervals in forced and unforced SEIR models, *Fields Inst. Commun.* **36** (2003), 33-45.

[8] N. T. J. Bailey, The Mathematical Theory of Infectious Diseases, 2nd ed., Hafner, New York, (1975).

[9] E. Bircan, J. H. Rob, Data visualization for time series in environmental epidemiology, Melbourne, (2001).

[10] F. Brauer, C. Castillo-Chavez, Mathematical Models in Population Biology and Epidemiology, Springer-Verlag, New York, Berlin, Heidelberg, (2000).

[11] C. Castillo-Chavez, Z. Feng, W. Huang, On the computation of $\mathcal{R}_0$ and its role on global stability, in C. Castillo-Chavez, with S. blower, P. van den Driessche, D. Kirschner, A. A. Yakubu (Eds), Mathematical Approach for Emerging and Reemerging Infectious Diseases: An Introduction, Springer, (2002), p. 229.

[12] Central Intelligence Agency World factbook, website: https://www.cia.gov/library/publications/the-world-factbook/index.html, accessed on November 12, (2008).

[13] C.D.C., Center for Disease Control and Prevention: Morbidity and Mortality, Weekly Report website: http://www.cdc.gov/mmwr/mmwr_wk/week_cvol.html, USA, accessed in March 2010.

[14] G. Chowell, Miller M. A. Miller, C. Viboud, Seasonal influenza in the United States, France and Australia, transmission and prospects, *Epidemiol. Infect.* **136** (2008), 852-864.

[15] C. Colijn, T. Cohen, M. Murray, Latent coinfection and the maintenance of strain diversity, *Bull. Math. Biol.* **71** (2009), 247-263.

[16] P. S. Cowpertwait, A. Metcalfe, Introductory Time series with R, Springer, New York, (2009).

[17] C. G. Cullen, An Introduction to Numerical Linear Algebra, Wadsworth, Inc., Boston, Massachusetts, (1994).

[18] O. Diekmann, J. A. P. Heesterbeek, J. A. J. Metz, On the definition and computation of the basic reproduction ratio $\mathcal{R}_0$ in models for infectious diseases, *J. Math. Biol.* **35** (1990), 503-522.

[19] K. Dietz, Epidemics and rumors: A survey, J. Roy *Statist. Soc. Ser. A* **130** (1967), 505-528.

[20] K. Dietz, The first epidemic model: A historical note on P. D. En'ko, *Austral. J. Statist.* 30A (1998), 56-65.

[21] O. Diekmann, Heesterbeek, J. A. P. Heesterbeek, Mathematical Epidemiology of Infectious Diseases, Model Building, Analysis and Interpretation, John Wiley and Sons, Ltd, Chichester, New York, Weinheim, Brisbane, Singapore, Toronto, (2000).

[22] A. d'Onofrio, On pulse vaccination strategy in the SIR epidemic model with vertical transmission, *Appl. Math. Lett.* **18** (2005), 729-732.

[23] P. V. D. Driessche, J. Watmough, Reproduction numbers and sub-threshold endemic equilibria for compartmental models of disease transmission *Math. biosci.* **180** (2002), 29-48.

[24] L. L. Dublin, A. J. Lotka, On the true rate of natural increase of a population, *J. Am. Stat. Assoc.* **20** (1925), 305-339.

[25] J. A. P. Heesterbeek, K. Dietz, The concept of $\mathcal{R}_0$ in epidemic theory *Stat. Neerl.* **50** (1996), 89-110.

[26] J. A. P. Heesterbeek, A brief history of $\mathcal{R}_0$ and recipe for its calculation *Acta Biotheret.* **50** (2002), 189-204.

[27] J. M. Heffernan, R. J. Smith, L. M. Wahl, Perspectives on basic reproduction ratio, *J. R. Soc. Interface* **2** (2005), 281-293.

[28] J. Doushoff, J. B. Plotkin, S. A. levin, D. J. Earn, Dynamical resonance can account for seasonality of influenza epidemics, P. Natl. Acad. Sci. USA **101** (2004), 16915-16916.

[29] S. M. Dunn, A. Constantinides., P. V. Moghe, Numerical Methods in biomedical Engineering, Elsevier Academic Press, (2006).

[30] Z. Feng, D. Xu, H. Zhao, The uses of epidemiological models in the study of disease control. Modeling and dynamics of infectious diseases, *Ser. Contemp. Appl. Math. CAM*, Higher Ed. Press, Beijing (2009), 150-166.

[31] Z. Feng, Final and peak epidemic sizes for SEIR models with quarantine and isolation, *Math. Biosci. Eng* **4** (2007), 675-686.

[32] B. F., Finkenstadt, B. T. Grenfell, Time series modeling of childhood diseases. A dynamical systems approach, *Appli. Stat.* **49** (2000), 182-205.

[33] C. J. Fu, L. Z. Lu, Exponential stability of SEIRS epidemic model with two delays, *J. Math. (Wuhan)* **28** (2008), 265-270.

[34] C. S. Gao, Z. Teng, D. Xie, The effects of pulse vaccination on SEIR model with two time delays, *Appl. Math. Comput.***201**(2008), 282-292.

[35] N. C. Grassly, C. Fraser, Seasonal infectious disease epidemiology, *Proc. R. Soc.* **273** (2006), 2541-2550.

[36] W. H. Hamer, Epidemic disease in England, *Lancet* **1** (1906), 733-739.

[37] H. W. Hethcote, The mathematics of infectious diseases, SIAM *Society for Industrial and Applied Mathematics* **42** (2000), 599-653 .

[38] J. Hou, and Z. Teng, Continuous and impulsive vaccination of SEIR epidemic models with saturation incidence Rates, *Math. Comput. Simulat.* **79** (2009), 3038-3054.

[39] J. Hou, H. Liu, Pulse vaccination in a delayed SEIR model with saturation incidence, *Int. J. Pure Appl. Math.* **49** (2008), 615-625.

[40] W. O. Kermack, A. G. McKendrick, Contributions to the mathematical theory of epidemics, part 1, *Proc. Roy. Soc. London Ser. A* **115** (1927), 700-721.

[41] A. Korobeinikov, Global properties of infectious disease models with nonlinear incidence, *Bull. Math. Biol.* **69** (2007), 1871-1886.

[42] A. Korobeinikov, Global properties of SIR and SEIR epidemic models with multiple parallel infectious stages, *Bull. Math. Biol.* **71** (2009), 247-263.

[43] R. Kuske, L. F. Gordillo, P. Greenwood, Sustained oscillations via coherence resonamce in SIR, *J. Theor. Biol.* **245** (2007), 259-469 .

[44] J. Ma, Z. Ma, Epidemic threshold conditions for seasonally forced SEIR models, *Math. Biosci. Eng.* **3** (2006), 161-172.

[45] D. Y. Melesse, A. B. Gumel, Global asymptotic properties of an SEIRS model with multiple infectious stages, *J. Math. Anal. Appl* **366** (2010), 202–217.

[46] G. McDonald, The analysis of equilibrium in malaria, *Trop. Dis. Bull.* **49** (1952), 813-829.

[47] J. D. Murray, Mathematical Biology, Biomathematics Texts 19, Berlin, Heidelberg, Springer Verlag, (1989).

[48] Y. Nakata, T. Kuniya, Global dynamics of a class of SEIRS epidemic models in a periodic environment, *J. Math. Anal. Appl.* **363** (2010), 230-237.

[49] D. Nokes, J. Swinton, The control of childhold viral infections by impulsive vaccination, *IMA J. Math. Appl. Boil. Med.* **12** (1995), 29-53.

[50] S. Rionero, On the nonlinear stability of the critical points of an epidemic SEIR model via a novel Liaponov function, *Rend. Accad. Sci. Fis. Mat. Napoli* **75** (2008), 115-129.

[51] R. Ross, The Prevention of Malaria, 2nd ed., John Murray, London, 1911.

[52] R Ross, H. P. Hudson, An application of the theory of probabilities to the study of the theory of pathometry, Part III, *Proc. Roy. Soc. London Ser. A* **43** (1917), 225-240.

[53] A. B. Sabin, Measles, killer of millions in developing countries: Strategy of elimination and continuation control, *Eur. J. Epidemiol.* **7** (1991), 1-22.

[54] W. M. Schaffer, T. V. Bronnikova, Parameter dependence in model epidemics. Non-contact rate-related parameters, *J. Biol. Dyn.* **1** (2007), 231-248.

[55] F. R. Sharp, A. J. Lotka, A problem in age distribution, *Phil. Mag.* **6** (1911), 435-438.

[56] S. H. Strogatz, Nonlinear Dynamics and Chaos with Applications to Physics, Biology, Chemistry and Engoneering, Perseus Books Publishing, LLC, Cambridge, (1994).

[57] E. Seier, Lecture Notes on Time Series Analysis, Personal Communication, (2010).

[58] G. Rost, J. Wu, SEIR epidemiological model wwith varying infectivity and infinite delay, *Math. Biosci. Eng.* **5** (2008), 389-402.

[59] C. Wei, L. Chen, A delayed epidemic model with pulse vaccination, *Discrete Dyn. Nat. Soc.* 2008, Art. ID 746951, 12 pp.

[60] J. Yuan, Z. Yang, Global dynamics of an SEI model with acute and chronic stages, *J. comput. Appl. Math.* **213** (2008), 465-476.

[61] Y. Nakata, T Kuniya, Global Dynamics of a Class of SEIRS Epidemic models in a Periodic Envoronment, *Journal of Mathematical Analysis and Applications* **363** (2010), 230-237.

[62] J. Zhang, Z. Ma, Global dynamics of an SEIR epidemic model with saturatinng contact rate, *Math. Biosci.* **185** (2003), 15-32.

[63] T. Zhang, Z. Teng, Pulse vaccination delayed SEIRS epidemic model with saturation incidence, *Appl. Math. Model.* **32** (2008), 1403-1416.

[64] T. Zhang, Z. Teng, On a nonautonomous SEIRS model in epidemiology, *Bull. Math. Biol.* **69** (2007), 1871-1886.

[65] T. Zhang, Z. Teng, Dynamic behavior of a delayed impulsive SEIRS model in epidemiology, *Rocky Mountain J. Math.* **38** (2008), 1841-1862.

[66] T. Zhang, J. Liu, Z. Teng, A non-autonomous epidemic model with time delay and vaccination, *Math. Meth. Appl.* **33** (2010), 1-11.

[67] Z. Zhao, L. Chen, X. Song, Impulsive vaccination of SEIR epidemic model with time delay and nonlinear incidence rate, *Math. Comput. Simul.* **79** (2008), 500-510.

VITA

ERIC NUMFOR

Education:	M.S. Mathematics, East Tennessee State University, Johnson City, Tennessee 2010
	M.S. Mathematics, University of Buea, Buea, Cameroon 2002
	B.S.(Hons.) Mathematics, University of Buea, Buea, Cameroon 1999
Professional Experience:	Graduate Teaching Assistant, East Tennessee State University, USA 2009–2010
	Assistant Lecturer, University of Buea, Cameroon 2007–2009
	Instructor, University of Buea, Cameroon 2003-2007
	Teacher, Christ the King College, Tiko Cameroon 2003-2006
	Graduate Teaching Assistant, University of Buea, Cameroon 2001–2003
Teaching:	East Tennessee State University, USA, Precalculus I, Summer 2010.
	University of Buea, Cameroon Mathematical Methods, 2007–2009 Mathematical Methods I B and II B 2004–2007
	Christ the King College, Tiko Cameroon Mathematics , Additional Mathematics and High School Mathematics and Statistics, 2003–2006
Author:	Pure Mathematics for Cameroon Schools, ANUCAM, 2007
	Ordinary Level Mathematics for Cameroon Schools, 2008.